The Institute for Solid State Physics
The University of Tokyo

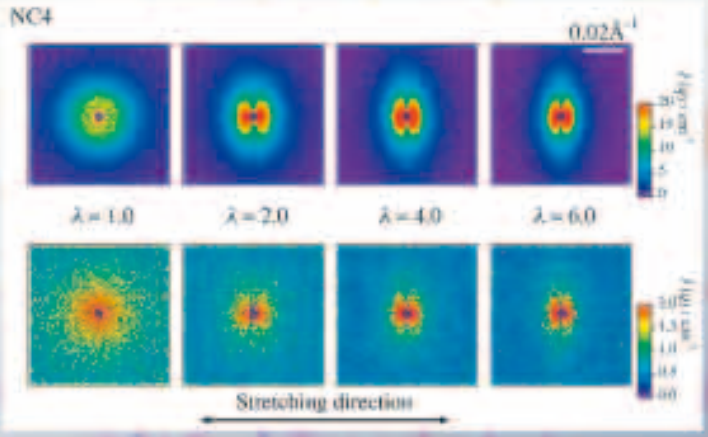

Activity Report 2006

Highlights of Joint Research
International Conferences and Workshops
ISSP Workshops

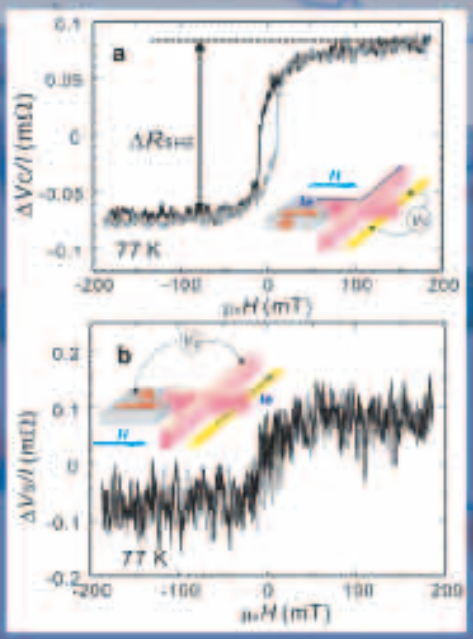

Activity Report: The Institute for Solid State Physics (ISSP) The University of Tokyo 2006

Highlights of Joint Research

Synchrotron Radiation Laboratory

The Synchrotron Radiation Laboratory (SRL) was established in 1975 as a research group dedicating to solid state physics using synchrotron radiation. In 1989, the SRL started to hold the Tsukuba branch, a branch laboratory in the Photon Factory (PF), High Energy Accelerator Research Organization (KEK). SRL maintains an undulator called Revolver, two beamlines and three experimental stations; BL-18A for angle-resolved photoemission spectroscopy and undulator beamlines, BL-19A and BL-19B for spin-resolved photoelectron spectroscopy and soft X-ray emission spectroscopy experiments, respectively. They are fully opened to outside users for experiments using high brilliant synchrotron radiation from the undulator. The operation time of these beamlines are about 5000 hours and the number of users is more than 200 a year.

The present SRL consists of the accelerator physics group and the solid state spectroscopy group. The members of the accelerator group have been carrying out research works on the accelerator physics and developing various new accelerator related technology in collaboration with other SR facilities. The spectroscopy group has been not only serving users at the Tsukuba branch with technical supports and advices, but also carrying out their own research works on advanced solid state spectroscopy.

In 2005, the operation of PF ring was quitted for six months to improve its characteristics as a light source. During this long-term shut down of PF, the staff members of SRL improved experimental apparatuses at the beamlines, which results some new achievements. They installed a new high resolution electron energy analyser (PHOIBOS 150) and an equipment for sample preparation at BL-19A. The new system is combined with high efficiency spin detector utilizing very low energy electron diffraction (VLEED) technique. After the completion of the new system, the apparatuses will be opened for spin-resolved photoemission experiments with a high energy resolution of several 10 meV and a figure of merit larger than 10^{-3} in the spin analysis.

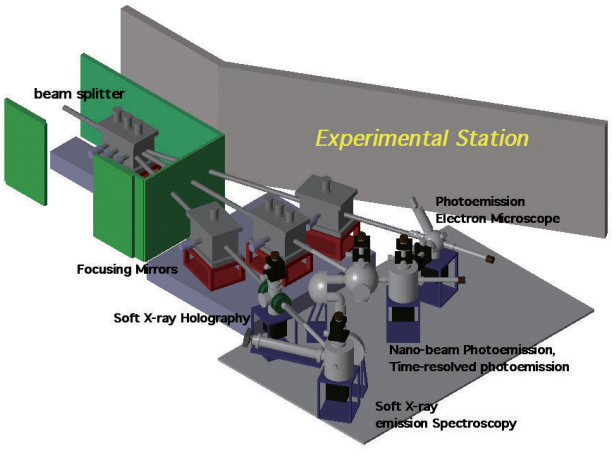

Fig. 1. Schematics of the undulator beamline at SPring-8

Since 1980s, SRL has been promoting the "Super-SOR" project for constructing a new synchrotron radiation facility with a third generation light source dedicated to the sciences in vacuum ultraviolet and soft X-ray (VSX) regions. However, in 2005 the president office of the University of Tokyo found out that the promotion of the project is very difficult since the budget for the new project is too big to be supported by a single university in Japan even after the reformation of the national universities. After many severe discussions, SRL has inclined to construct beamlines using undulator radiation in other SR facilities instead of constructing the facility with a light source and to promote advanced materials sciences using high brilliance and small emittance of SR which have been considered in the Super-SOR project.

In October 2006, the president office decided to promote research activities of the University of Tokyo using SR, and unified them under a new group, the Synchrotron Radiation Research Organization (SRRO) of the University of Tokyo. The new Organization consists of two divisions, Materials Science Division and Life Science Division. The staff members of SRL, the solid state spectroscopy group will participate to the Materials Research Division and play essential roles in promoting scientific activities using SR. The University also supports them financially and she will be ready to prepare the budget for the construction of new beamlines in existing SR facilities. SRRO is planning to construct a new 25m-long undulator at SPring-8. They also proposed new beamlines and experimental equipments using high brilliance synchrotron radiation in soft X-ray region. They are those for soft X-ray microscopy experiments, time-resolved experiments which will only be possible using third generation light source and will promise us a considerable progress in the studies of nano-particles and real time observation of magnetic domains and of chemical reaction at catalytic surfaces, etc.

The accelerator group started to study ERL(energy recovery linac)-based light sources and develop ERL components in collaboration with KEK and JAEA. A nine-cell superconducting cavity was designed for high current ERLs and will be fabricated and tested in 2007. A high-power input coupler with two ceramic windows and a novel HOM-damped structure for suppression of both dipole and quadrupole modes are also being designed for the cavity. Furthermore multi-bunch beam break-up due to long-range resistive-wall wake-fields that could be a serious problem for high-current ERLs was intensively investigated to fully understand and cure it. They also developed several advanced components and methods related to light source accelerators. A copper-coated stainless-steel vacuum chamber was experimentally demonstrated to work well under the ultra-high vacuum and its copper-coating technique was adopted for a new BL-16 undulator chamber at KEK-PF to keep the beam stable by reducing the resistive-

wall wakefield. A pulse sextupole magnet for normal and top-up injections was designed and confirmed by simulations to inject the beam into the PF-ring without serious beam loss. A digital beam position monitor system was developed to stabilize low-emittance beam positions with high resolution and flexibility. Its performance test was successfully carried out with a test bench at ISSP and then the system was also demonstrated by a beam test at KEK-LINAC to be useful for single-pass beam position measurements.

Neutron Science Laboratory

The Neutron Science Laboratory (NSL) has been playing a central role in neutron scattering activities in Japan since 1961 by performing its own research programs as well as providing a strong general user program for the university-owned various neutron scattering spectrometers installed at the JRR-3 operated by Japan Atomic Energy Agency in Tokai. In 2003, the Neutron Scattering Laboratory was reorganized as the Neutron Science Laboratory to further promote the neutron science with use of the instruments in JRR-3. Under the general user program supported by NSL, 14 university-group-owned spectrometers in the JRR-3 reactor (20MW) are available for a wide scope of researches on material science, and proposals close to 300 are submitted each year, and the number of visiting users under this program reaches over 6000 person-day/year.

Triple axis spectrometers and a high resolution powder diffractometer are utilized for a conventional solid state physics and a variety of research fields on hard-condensed matter, while in the field of soft-condensed matter science, researches are mostly carried out by using the small angle neutron scattering (SANS-U) and/or neutron spin echo (iNSE) instruments. The upgraded time-of-flight (TOF) inelastic scattering spectrometer is now opened to the user proposals.

Major research topics on the hard-condensed matter science cover stripe order in high-T_c superconductors, and closely related 2 dimensional systems, charge and orbital ordering in CMR manganites, quadrapolar ordering in rare-earth based intermetallic compounds, spin dynamics of low dimensional dimmer systems, etc. On the other hand, the research topics on the soft-condensed matter science cover structural characterization of polymer blends, micelles, amphiphilic polymers block copolymers, liquid crystals, proteins, inorganic gels, dynamics of brush-polymers on surface, slow dynamics of surfactants, pressure dependence of dynamics of amphiphilic membranes, and so on. In addition, there are a variety of activities on fundamental physics, neutron beam optics, developments of neutron scattering techniques.

The NSL also operates the U.S.-Japan cooperative program on neutron scattering, providing further research opportunities to material scientists who utilize the neutron scattering technique for their research interests.

The details of individual studies and research highlights in JFY2006 will be reported in the NSL-ISSP Activity Report vol. 14.

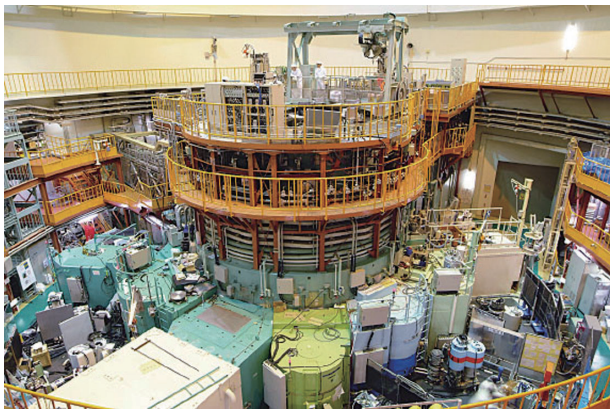

Fig. 1. The reactor hall of JRR-3. The eight neutron scattering instruments are attached to the horizontal beam tubes in the reactor experimental hall. Two thermal and three cold guides are extracted from the reactor core towards the guide hall located to the left.

Supercomputer Center

The mission of the Supercomputer Center of the Institute (SCC-ISSP) is to serve the whole community of computational condensed-matter physics in Japan providing it with high performance computing environment. The mission is achieved through the User Programs supervised by the Materials Design and Characterization Laboratory (MDCL). One of our specific goals is to selectively promote and support large-scale computations.

The center operates two super-computers, systems A and B, which were renewed in March 2005. System A is Hitachi SR11000/48 that consists of 48 high performance nodes composed of tightly-coupled microprocessors. A node can be used as if it were a single-processor computer by automatic parallelization of its FORTRAN compiler. System A has 2.8 TB memory and archives 5.8 TFlops peak performance in total. On the other hand, System B, which is SGI Altix 3700/1280, is a loosely-coupled parallel supercomputer consisting of 19 nodes inter-connected by a gigabit Ethernet network. Each node is a distributed-shared-memory-type computer consisting of 64 Intel Itanium 2 CPUs interconnected by a rather high performance network and have 64 GB memory. System B achieves 7.7 TFlops total throughput performance.

Any staff member of university faculties or public research institutes in Japan can apply for a project of the User Program. Proposals are evaluated by the Steering Committee of the center, under which the Supercomputer Project Advisory Committee is formed to review proposals in detail. In fiscal year 2006 totally 184 projects were approved. The total points applied and approved are listed in Table. 1 below.

Class	Max/Min Point	Application	# of Proj.	Total points (K points) Applied Sys-A	Applied Sys-B	Approved Sys-A	Approved Sys-B
A	<100K	any time	2	150	50	150	50
B	<2M	twice a year	52	60100	39350	57600	38250
C	<20M	twice a year	112	1176200	757200	930700	684500
D		any time	17	265000	218000	173400	177000
S	>20M	twice a year	1	0	70000	0	70000
Total			184	1501450	1084600	1161850	969800

Table 1. Research projects approved in 2006.
The maximum points allotted to the project of each class are the sum of the points for the two systems. 1 K points of System-A correspond to charge for 0.37 hours × node, while the corresponding figure is 0.22 hours × node for System-B.

The research projects are roughly classified into the following three categories (the number of projects approved):

First-Principles Calculation of Materials Properties (71)
Strongly Correlated Quantum Systems (66)
Cooperative Phenomena in Complex, Macroscopic Systems (47)

All the three involve both methodology of computation and its applications. The results of the projects are reported in 'Activity Report 2006' of the SCC-ISSP. In the report the following four invited articles are included:

"Giant Intrinsic Spin Hall Effect in Transition Metal Compounds", by H. Kontani, T. Tanaka, D. S. Hirashima, K. Yamada, and J. Inoue,
"Fluctuations near Quantum Critical Points of Valence Transition and Superconductivity", by S. Watanabe,
"A First-principles Investigation on the Mechanism of Nitrogen Dissolution in the Na Flux Method", by M. Kawahara, S. Yanagisawa, and Y. Morikawa,
"Chaos Effect in the Edwards-Anderson Ising Spin Glass: A numerical Domain Wall Renormalization-Group Study", by M. Sasaki, K. Hukushima, H. Yoshino, and H. Takayama.

International MegaGauss Science Laboratory

The mega-gauss facility at the Institute for Solid State Physics has decided to introduce a 210 MJ flywheel generator which is the world largest DC power supply (recorded in Guinness book of records in 1907/98) for generation of the long-pulse magnetic field, and to transfer it from Naka Fusion Institute, Japan Atomic Energy Agency. The DC power generator finished its role of supplying energy into the Toroidal magnetic field coil in JFT-2M (JAERI Fusion Torus-2M) tokamak nuclear fusion testing device in 2004.

In accordance with this decision, which is recommended by the High Magnetic Field Forum Japan, we have changed the structure of our organization of the previous group and named it the “International MegaGauss Science Laboratory (IMGSL)”. This laboratory started from 2006 fiscal year.

The aim of this laboratory is to study the physical properties of solid-state materials (such as semiconductors, magnetic materials, metals, insulators, superconducting materials) under ultra-high magnetic field conditions. Such a high magnetic field is also used for controlling the new material phase and functions. Our pulse magnets, at moment, can generate up to 80 Tesla by non-destructive manner (the world record), and from 100 up to 630 Tesla (the world strongest as an in-door record) by destructive (the single turn coil and the electro-magnetic flux compression) methods.

They are opened to scientists both from Japan and from overseas, especially from Asian countries, and many fruitful results are expected to come out not only from collaborative research but also from our in-house activities. One of our ultimate goals is to provide the scientific users as our joint research with magnets capable of a 100 T, milli-second pulses in a non-destructive mode, and to offer physical precision measurements. The available measuring techniques now involve magneto-optical measurements, cyclotron resonance, spin resonance, magnetization and transport measurements.

Our interests cover the study on quantum phase transitions (QPT) induced by high magnetic fields. Field-induced QPT has been explored in various materials such as quantum spin systems, strongly correlated electron systems and other magnetic materials. Non-destructive pulsed fields enable us to measure many kinds of materials precisely. The number of collaborative groups for the research is over 30 in the year of 2006. Multiple extreme physical conditions combined with ultra-low temperatures and ultra-high pressures are also available. The magnet technologies are intensively devoted to the quasi-steady long pulse magnet (an order of 1-10 sec) energized by the giant DC power supply, and also to a 100 Tesla nondestructive magnet.

Our destructive magnets, such as the single-turn coil and the electro-magnetic flux compression (EMFC) systems, would be oriented toward easier access and more reliable measurements for solid-state physics than previously obtainable. One of our recent successes was the achievement of over 630 T within a 3.8 MJ energy injection by the EMFC, in which a new type of primary coil with a simpler design was employed. These are oriented for developing new horizons in material science realized under such extreme quantum limit conditions.

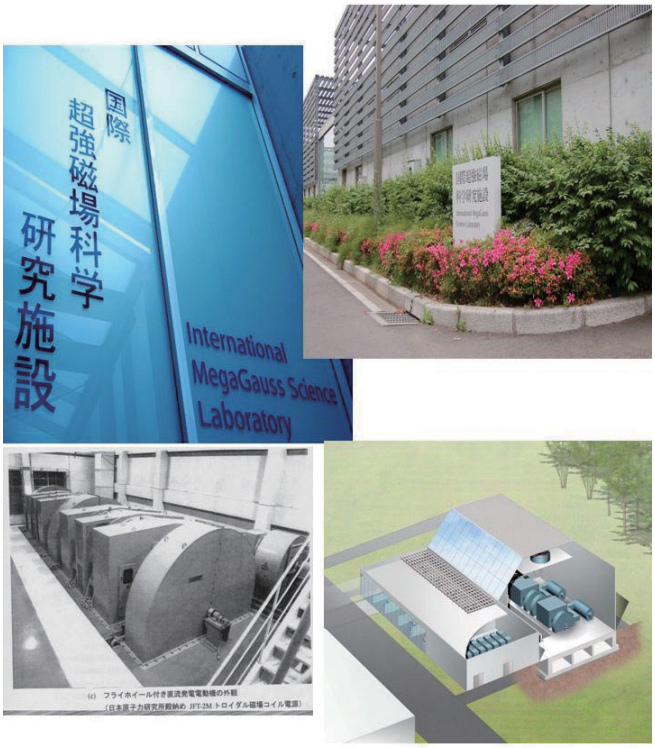

Fig. 1. Entrance signboards of the new International MegaGauss Science Laboratory. The fly-wheel generator which is the world largest DC power supply for non-destructive pulse magnets aiming at generating 100 Tesla (right bottom). Birds-eye-view of the long-pulse magnet building in which the fly-wheel generator with magnet stations are to be installed (left bottom).

NMR Evidence for a Totally Symmetric Order Parameter in $PrFe_4P_{12}$

J. Kikuchi and M. Takigawa

Intermetallic compounds with the filled-skutterudite structure RT_4X_{12} (R = rare earth, T = transition metal, X = pnictogen) has attracted strong recent attention because of a variety of intriguing phenomena in a common crystal structure (Fig. 1 left) such as metal-insulator transitions, multipole orders, exotic superconductivity, and anomalous phonons [1]. Among them, $PrFe_4P_{12}$ shows a peculiar phase transition at T_A=6.5K. The low temperature (T) phase has no spontaneous magnetic moment at zero field and is suppressed by a magnetic field of 4 - 7 T depending on the field directions (Fig. 1 right). The low-T phase has a structural modulation with the wave vector $\boldsymbol{Q}$=(1,0,0), indicating loss of t(1/2, 1/2, 1/2) translation. Distinct electronic states for two Pr^{3+} ions in the bcc unit cell observed by resonant X-ray scattering, the field-induced staggered magnetization observed by neutron scattering, and elastic anomalies have all suggested an antiferro-quadrupole order likely to be of Γ_{23}-type. However, direct identification of the order parameter has not been made yet.

We have performed nuclear magnetic resonance (NMR) experiments on ^{31}P nuclei for microscopic understanding of the low-T ordered phase [2]. We observed that all NMR lines in the high-T phase split into two upon entering into the low-T phase (Fig. 2) irrespective of the field direction. This

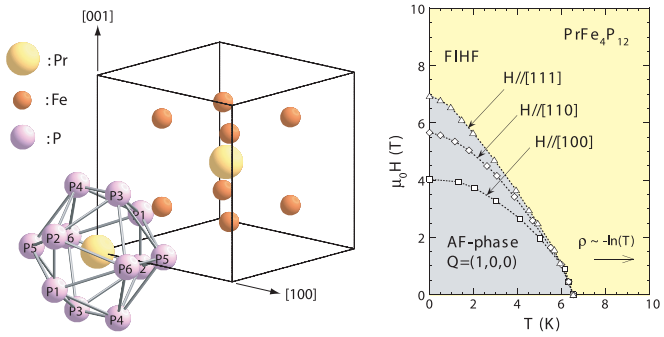

Fig. 1. Crystal structure (left) and the phase diagram (right) of $PrFe_4P_{12}$.

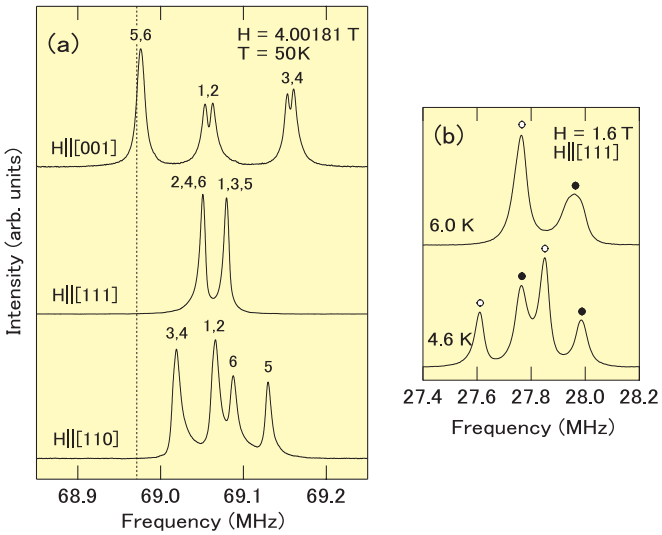

Fig. 2. (left) ^{31}P NMR spectra at T=50 K. The numbers indicate assignment of each peak to the P sites (P1 - P6, see Fig. 1 left). (right) ^{31}P NMR spectra at 6.0 K (above T_A) and at 4.6 K (below T_A) for the field of 1.6 T along [111]. NMR peaks from P1, P3, and P5 sites (P2, P4 and P6 sites) are shown by solid (open) circles.

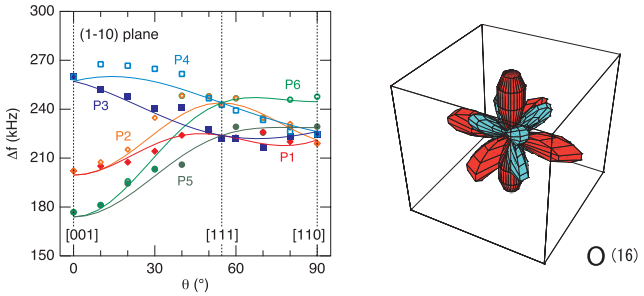

Fig. 3. (left) The angle dependence of the NMR line splitting in the low-T phase (T=4.2 K, H=1.6 T). The lines are fitting to the phenomenological model described in ref. [3]. (right) Schematic illustration of a totally symmetric hexadecapole moment. Note that the cubic symmetry is preserved in spite of a highly anisotropic charge distribution.

should be ascribed to the distinction between two P_{12} cages surrounding Pr sites at the corner and the body center of the original *bcc* lattice. Absence of any additional line splitting indicates that the 4f-electronic charge distribution of each Pr sites preserves the T_h point symmetry of the high-T phase. From group theoretical arguments [3] and phenomenological fitting of the angle dependence of the splitting (Fig. 3 left) [4], we have established that the order parameter belongs to the totally symmetric Γ_1 representation, ruling out any type of quadrupole order. The line splitting vanishes as the magnetic field is reduced to zero, indicating that the primary order parameter at zero field is electric, that is even-rank multipole moments. For Pr^{3+}, the lowest order totally symmetric even-rank multipole is the hexadecapole shown in Fig. 3 (right).

What is the driving force for such a peculiar order ? A hint is provided by the band structure calculation showing a nesting feature of the conduction band with $\boldsymbol{Q}$=(1,0,0) [4]. It is well known that electron-lattice coupling in the presence of Fermi surface nesting leads to a charge density wave order. A similar Fermi surface instability can be induced by coupling between conduction electrons and 4f multipole moments. $PrFe_4P_{12}$ may be an example of such a novel type of order.

References

[1] Y. Kuramoto, JPJS Online-News and Comments [Apr. 13, 2007].
[2] J. Kikuchi, M. Takigawa, H. Sugawara, and H. Sato, J. Phys. Soc. Jpn. **76**, 043705 (2007) (Selected for JPSJ Editor's Choice).
[3] O. Sakai, J. Kikuchi, R. Shiina, H. Sato, H. Sugawara, M. Takigawa, and H. Shiba, J. Phys. Soc. Jpn. **76**, 024710 (2007).
[4] H. Harima and K. Takegahara, J. Phys.: Condens. Matter **15**, S2081 (2003).

Authors

J. Kikuchi[a], M. Takigawa, H. Sugawara[b,c], H. Sato[c], O. Sakai[c], R. Shiina[c], and H. Shiba[d],
[a]Department of Physics, Meiji University
[b]Faculty of Integrated Arts and Science, University of Tokushima
[c]Graduate School of Science, Tokyo Metropolitan University
[d]The Institute of Pure and Applied Physics

Fast Molecular Transport in Hydrogen Hydrates by High-Pressure Diamond Anvil Cell NMR

T. Okuchi, M. Takigawa, and T. Yagi

Properties of molecular materials change with pressures. At several to several tens of gigapascal, chemical bonding may transform its fundamental nature. Water ices and gas

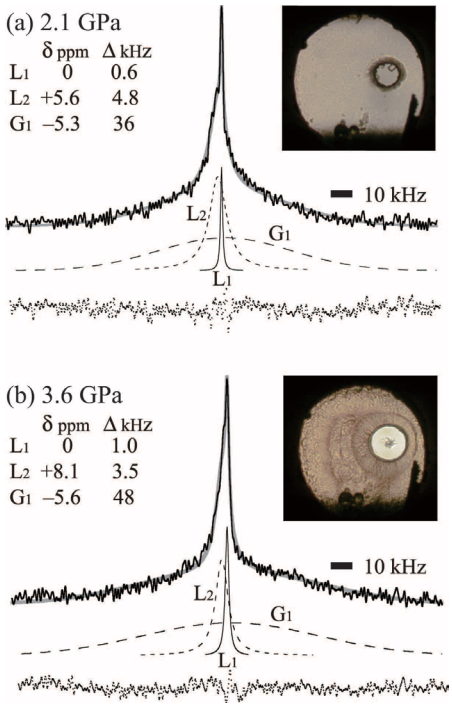

Fig. 1. Solid-echo powder NMR spectra at 300 MHz and optical micrograph of the hydrogen hydrates synthesized within the diamond anvil cell at high pressures. For each figure, the upper part shows the observed spectrum and its fitting curve, the middle part shows model fitting peaks, and the lower part shows the residual. (a) The filled-ice II phase. (b) The mixture of filled-ice Ic and pure ice VII phases. The L_1 peak shows highly-mobile H_2 guest molecules enclosed within the ice frameworks. The L_2 and G_1 peaks show moderately mobile and static H species within the H_2O framework.

hydrates are typical examples that involve flexible hydrogen-bonding phenomena and, therefore, particularly sensitive to the pressure. Their structure and transportation properties at this pressure regime are not only important by itself but also giving implications for internal structure and material transport of icy giant planets and icy satellites in the solar system. We investigated hydrogen hydrates which are typical examples of these ice materials, using a novel method to analyze both molecular structure and motion at high pressure-high-resolution diamond-anvil-cell nuclear magnetic resonance spectroscopy [1].

A distinct feature of H_2 is its smallest size among the molecules. It is smaller than intrinsic interstices of some ice polymorphs. At pressures higher than 0.4 GPa, H_2 spontaneously dissolve into these ice frameworks to produce dense

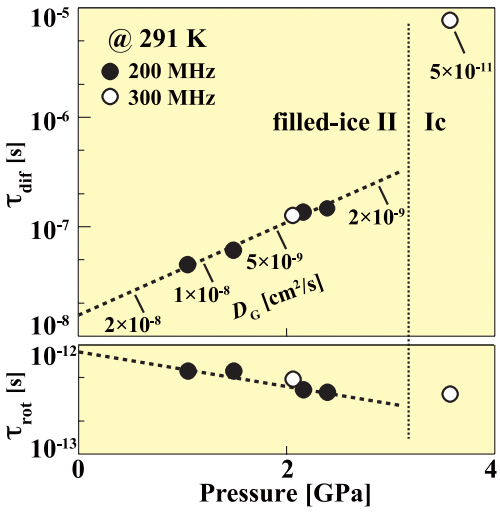

Fig. 2. Two motional correlation times (τ_{rot} and τ_{dif}) and diffusion coefficient (D_G) of the guest H_2 molecules. They are determined from pressure and frequency dependences on T_1^{-1} and T_2^{-1} of the guest H_2.

hydrogen hydrates [2]. These hydrates have the structures of ice II and Ic , hence they are called as filled ice hydrates. The filled-ice II hydrate (C_1) is stable to 3 GPa with a composition H_2:H_2O = 1:6. The filled-ice Ic hydrate (C_2) is stable to at least 60 GPa with H_2:H_2O = 1:1.

In situ proton NMR spectra of these filled-ice hydrogen hydrates at pressures reveal fast translational motion of the H_2 molecules enclosed within the ice frameworks. The NMR spectra to 3.6 GPa gave sharp resonances of the H_2 guests, revealing liquid-like mobile nature of the guest H_2 (Fig. 1). Pressure effects on T_1^{-1} and T_2^{-1} of the H_2 indicate that molecular rotation and diffusion contribute together to the spin relaxation, from which two motional correlation times τ_{rot} and τ_{dif} of the guest H_2 were determined separately (Fig. 2). A liquid-like large diffusion coefficient of the H_2 with little pressure sensitivity was deduced from τ_{dif}, indicating that the ice framework allows active guest translation even in extensively compressed states.

References
[1] T. Okuchi, Phys. Earth Planet. Inter. **143-144**, 611 (2004).
[2] W. L. Vos, L. W. Finger, R. J. Hemley, and H. K. Mao, Phys. Rev. Lett. **71**, 3150 (1993).
[3] T. Okuchi, M. Takigawa, J. Shu, H. K. Mao, R. J. Hemley, and T. Yagi, Phys. Rev. B. **75**, 144104 (2007).

Authors
T. Okuchi[a], M. Takigawa, J. Shu[b], H. K. Mao[b], R. J. Hemley[b], and T. Yagi
[a]Nagoya University
[b]Carnegie Institution of Washington

Localization Problem in the Quasiperiodic System with the Spin Orbit Interaction

M. Kohmoto, D. Tobe, and C. Wexler

The quasiperiodic systems are intermediate between periodic and random. Electronic states are always extended in periodic systems. In one dimension, states are always localized in random systems. The one-dimentional quasiperiodic systems show various interesting wave function and energy spectral character [1].

We study one-dimensional quasiperiodic system obtained from the tight-binding model on the square lattice in a uniform magnetic field with the spin orbit interaction. The problem involves a Hamiltonian:

$$H = -\sum_{<i,j>} t_{ij} c_j^{\dagger} c_i e^{i\theta_{ij}^{x}} + \lambda_R (i \sum_{n,m} c_{n,m+1}^{\dagger} \sigma_x c_{n,m} e^{i\theta_{n,m}^{y}} - i \sum_{n,m} c_{n+1,m}^{\dagger} \sigma_y c_{n,m} e^{i\theta_{n,m}^{x}}) + \text{H.c.},$$

where λ_R is the Rashba spin orbit coupling. The phase diagram with respect to the Harper coupling and the Rashba coupling are proposed from a number of numerical studies including a multifractal analysis. (Fig.1).

There are four phases, I, II. III, and IV in this order from weak to strong Harper couplings. In the weak coupling phase I all the states are extended, in the intermediate coupling phases II and III mobility edges exist and accordingly localized and extended states coexist, and in the strong Harper coupling phase IV all the states are localized. Phases I and IV are related by the duality and also phases II and III are related by the duality. A localized state is related to an extended state by the duality and vice versa. The boundary

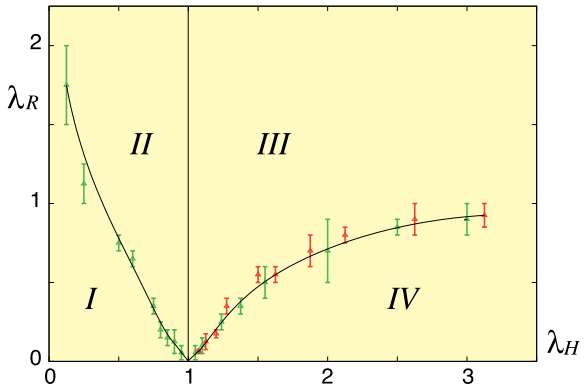

Fig. 1. Proposed phase diagram. The critical line between II and III is $\lambda_H \equiv t_y / t_x = 1$.

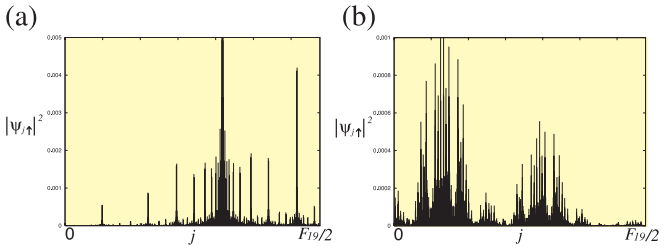

Fig. 2. Plots of the wave functions with $\sigma = \uparrow$ on the self-dual critical line (a) at the edge of the spectra, (b) at the center of the spectra. $(\lambda_H,\lambda_R) = (1.0,1.0)$. $q = F_{19} = 6795$.

between phases II and III is the self-dual line on which all the states are critical. Our result gives a counter example of the proof of pure spectrum by Aubry duality. Critical wave functions on the self-dual critical line are shown in Fig. 2.

References
[1] H. Hiramoto and M. Kohmoto, Int. J. Mod. Phys. B **6**, 281 (1992).

Authors
M. Kohmoto, D. Tobe, and C. Wexler[a]
[a]University of Missouri-Columbia

A Constrained First-Principles Molecular Dynamics Approach to Electron-Transfer Reactions in Solution

Y. Tateyama

Chemical reactions with electron-transfer in solution, so called "redox reactions", play crucial roles in diverse topics such as battery, fuel cell, catalysis, corrosion, photosynthesis. Fundamental aspects of redox reactions are usually characterized by free-energies. Free-energies have been intensively calculated using the constrained first-principles molecular dynamics (FPMD) methods, but those methods assume that the number of electrons is unchanged during the reaction and the surrounding bond network is only weakly perturbed by the reaction. Therefore they cannot be applied to the redox reactions.

To generalize the constrained FPMD method and make the redox reactions a target of the study, we have developed novel computational methods [1, 2]. In particular, the '(blue-moon ensemble) constrained FPMD energy gap method' [2] can deal with free-energy difference between the states with different charges as well as the different chemical bond networks taking thermal fluctuations of solute and solvent into account. Since the method is derived using fundamental

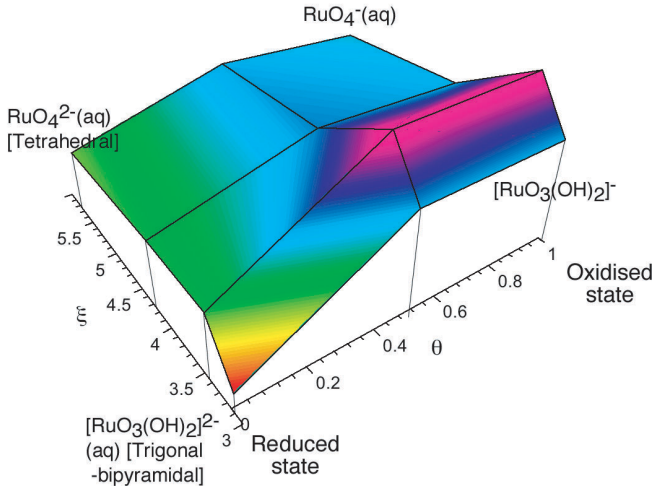

Fig. 1. Helmholtz free energy profile of the redox reaction, $RuO_4^- + H_2O + e^- \rightarrow [RuO_3(OH)_2]^{2-}$. The symbols, ξ and θ, denote the reaction coordinates with respect to the chemical bond change (between tetrahedral and trigonal-bipyramidal forms) and the electron transfer (between oxidised and reduced states), respectively. The overall reaction free energy is calculated to be -0.65 eV, which is in good agreement with the experimental value (-0.59 eV). Owing to the lower activation free energy, the reaction pathway via RuO_4^{2-} is more favourable than that through $[RuO_3(OH)_2]^-$.

principles of quantum mechanics and statistical physics only, it should be applicable under much broader contexts.

We have applied it to a water cleavage reaction coupled to electron transfer on a transition metal oxide ion in aqueous solution and demonstrated that it can well reproduce the experimentally determined free-energies. The resultant free-energy profile is shown in Fig. 1. We consider that this will open new perspectives for first-principles investigation of electron transfer reactions coupled to chemical bond breaking/formation.

References
[1] Y. Tateyama, J. Blumberger, M. Sprik, and I. Tavernelli, J. Chem. Phys. **122**, 234505 (2005).
[2] Y. Tateyama, J. Blumberger, T. Ohno, and M. Sprik, J. Chem. Phys. **126**, 204506 (2007).

Authors
Y. Tateyama[a]
[a]National Institute for Materials Science

An Atomic Seesaw Switch for One-Dimensional Electrons on Ge (001)

A. Ishii and F. Komori

Reversible switching of electronic conduction through atom manipulation is one of the main subjects of nanoscience. However, different conducting pathways have not been clearly observed with atomic resolution. We demonstrate the correlation between the change of surface atomic position and that of the reflection of one-dimensional (1D) surface-state electrons on the Ge (001) surface with a low coverage of Sn atoms [1].

On the clean Ge(001) surface, two atoms form a buckled dimer, and bonding π- and antibonding π^*-states localize on upper and lower atoms of the dimer. The Ge dimers align in the [110] direction and form a dimer row. The π^*-electron behaves like a 1D free electron along the dimer row (see Fig. 1). The buckling orientation of the Ge dimer can be reversibly controlled by surface bias voltage of STM below

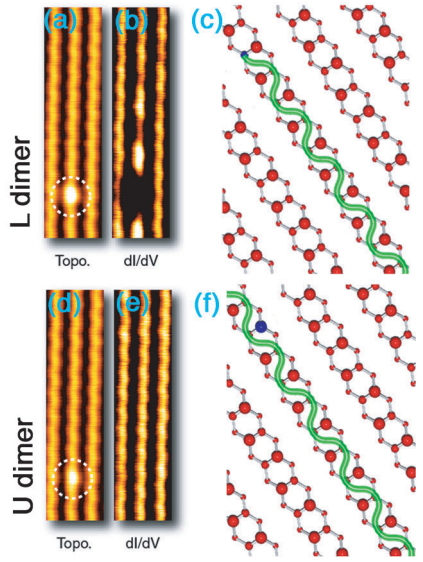

Fig. 1. (a,b) Topographic (a) and dI/dV (b) images of the Ge(001) surface with L dimer at 80 K. The L dimer is imaged as a protrusion in the topographic image, and a standing wave is observed around the L dimer in the dI/dV image. (c) Schematic illustration showing the π^*-electrons (green line) , which conduct on the lower atoms of the Ge dimers in the dimer row directon [110], are reflected by the Sn atom (small blue ball) at the lower dimer position. Red balls indicate the Ge atoms. Large balls are the upper dimer atoms, and small ones the lower. (d,e) Topographic (d) and dI/dV (e) images of the Ge(001) surface with the U dimer at 80 K. The U dimer is imaged as a protrusion in the topographic image while no standing wave is observed around the U dimer in the dI/dV image. (f) Schematic illustration showing the π^*-electrons (green line) can go through the Sn-Ge dimer. The Sn atom (large blue ball) at the upper dimer position little affects the π^*-electron conduction.

80 K [2].

When Sn atoms are deposited on the clean Ge(001) surface at room temperature, buckled dimers originating from the Sn atoms are formed at the Ge dimer position in the surface [3]. The contrast of the STM dimer image at 80 K changes by reversing its buckling orientation as shown in Fig. 2. Thus, it is identified as a heterogeneous Sn-Ge dimer. On the basis of first-principles calculations, the optimized structure of the heterogeneous dimers is estimated. The most stable structure is the buckled dimer with the Sn atom at the upper dimer position (U dimer). The energy of the dimer with the Sn atom at the lower dimer position (L dimer) is 60 meV higher than the ground state.

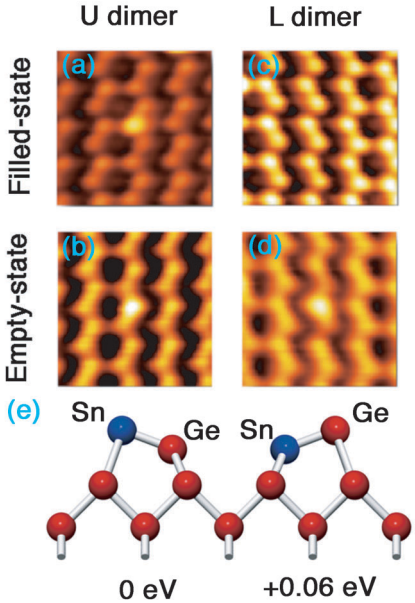

Fig. 2. (a-d) Filled (V_b = – 0.5 V) and empty (V_b = + 0.5 V) state STM images for the Sn-Ge dimers with the Sn atom at the upper (U dimer) and lower (L dimer) positions on the Ge(001) surface. Brightly imaged protrusions indicating the Sn-Ge dimer are seen in (a,b,d) while its image is the same as the Ge-Ge dimer in (c). Local superstructure of the surface changed by reversing the buckling orientation of the Sn-Ge dimer. (e) Structural models of the U dimer and the L dimer. The energy of the L dimer is 0.06 eV higher than that of the U dimer.

An atomic seesaw switch is realized for the 1D π^* electrons in the Ge dimer-row direction by using STM to flip reversibly the buckling orientation of a single Sn-Ge dimer in the dimer row at 80 K. When the Sn atom of the heterogeneous dimer is at the lower position (L dimer), the 1D electrons are reflected and a standing wave of this state is observed in the dI/dV image as in Fig. 1(b). Whereas, when it is at the upper position (U dimer), the 1D electrons pass through the heterogeneous dimer, and no standing wave is observed as in Fig. 1(e). In this state, the lower atom of the dimer is Ge, and the π^* state of the dimer is little different from that of the Ge-Ge dimers.

References

[1] K. Tomatsu *et al*., Science **315**, 1696 (2007).
[2] Y. Takagi *et al*., J. Phys. Soc. Jpn. **72**, 2425 (2003).
[3] K. Tomatsu *et al*., Surf. Sci. **601,** 1736 (2007).

Authors

K. Tomatsu, K. Nakatsuji, T. Iimori, Y. Takagi, H. Kusuhara[a], A. Ishii[a], and F. Komori

[a]Dep. Appl. Math. and Phys., Tottori University

STM and STS Studies of a Surface-new-material: Silicon Oxynitride Ultrathin Film Formed on 6H-SiC(0001)

H. Tochihara and F. Komori

Uniform, abrupt interface between insulating layer and semiconductor surface has been a long-standing requirement for progress of electronic devices. Silicon carbide (SiC) is a promising semiconductor for next-generation power devices due to its fundamental properties [1]. However, oxides/SiC interface produced by conventional methods has a variety of defects with high concentration. Very recently, Shirasawa *et al.* have succeeded to prepare a dangling-bond-free, ordered

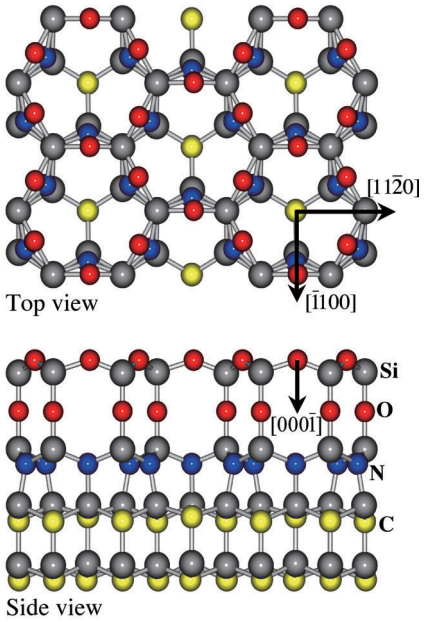

Fig. 1. Top and side views of ball and stick model of the SiON film on 6H-SiC(0001).

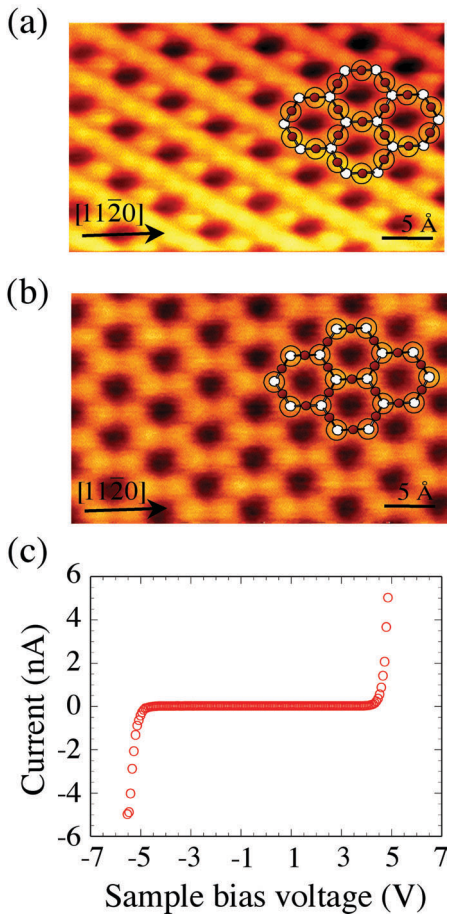

Fig. 2. (a) filled- and (b) Empty-state STM images of the SiON film taken at sample bias voltages of (a) -5.0 and (b) 4.5 V. Transparent circles indicate the bright protrusions. Ball and stick model of the silicate layer of the SiON is overlaid, where white and red spheres are Si and O atoms, respectively. (c) A typical *I-V* characteristic in STS measurement on the SiON film.

silicon oxynitride (SiON) epitaxial ultrathin film on a 6H-SiC(0001) surface [2]. Its atomic structure determined by means of a dynamical low-energy electron diffraction (LEED) analysis is shown in Fig. 1. The SiON film has a hetero-double-layer structure: a silicon dioxide monolayer on a silicon nitride monolayer via Si-O-Si bridge bonds. The SiON film is grown on the unreconstructed SiC(0001) surface with the atomically abrupt interface. Furthermore, since each O and N atom binds to two and three Si atoms respectively, and all Si atoms are four-coordinated, there are no dangling bonds in the unit cell. Actually, the SiON film is very stable even in air!

High-resolution scanning tunneling microscopy (STM) and spectroscopy (STS) have been successfully applied to the insulating SiON ultrathin film [2]. Atom-resolved filled- and empty-state STM images of the same area support the atomic arrangement of the silicon dioxide layer of the SiON in Fig. 2(a) and (b), respectively, where ball and stick model of the silicon dioxide layer is overlaid and protrusions in the images are outlined by transparent circles for clarification. It is clearly seen that the bright protrusions are positioned at different sites between filled- and empty-state images. In bulk SiO_2 and Si_2N_2O, density of states (DOS) of the conduction band is mostly originated from Si orbitals, and near the valence band maximum O 2*p* orbitals have prominent DOS. Thus, we can conclude that the protrusions in the filled- and empty-state images correspond to O and Si atoms, respectively. It is surprising that STS *I-V* characteristic measured on the silicon dioxide layer in Fig. 2(c) shows almost the same value of band gap as that of bulk SiO_2, ~9 eV. This is probably due to a strong resemblance of structural parameters such as Si-O bond length and Si-O-Si bond angle between the silicate layer of the SiON and SiO_2 crystals. This fact suggests that underlying silicon nitride single layer also has a similar value of band gap with that of bulk silicon nitrides, ~5 eV. Thus, it is an interesting issue to study the band gap and band offset in the hetero-double-layer structure.

References
[1] W. J. Choyke, H. Matsunami, and G. Pensl, *Silicon Carbide Recent Major Advances* (Springer, Germany, 2004).
[2] T. Shirasawa, K. Hayashi, S. Mizuno, S. Tanaka, K. Nakatsuji, F. Komori, and H. Tochihara, Phys. Rev. Lett. **98**, 136105 (2007).

Authors
T. Shirasawa[a], K. Nakatsuji, F. Komori, and H. Tochihara[a]
[a]Dept. Mol. & Mat. Sci., Kyushu University

Spin Pumping effect in Superfluid ^{3}He A_1 phase

H. Kojima and H. Ishimoto

When liquid ^{3}He is cooled down to low enough temperatures in a magnetic field, the normal liquid first makes a transition into superfluid A_1 phase at T_{c1} and then into superfluid A_2 phase at a lower temperature T_{c2}. The most important aspect of the A_1 phase is that its superfluid component is totally spin-polarized along the magnetic field. It is a kind of ferromagnetic superfluid. A mass superflow is then simultaneously a spin flow. The phase transition into the A_1 phase is accompanied by the spontaneous breaking of relative spin-gauge symmetry. Interesting hydrodynamic effects occur in the A_1 phase such as a unique magnetic fountain pressure effect which was predicted by Liu [1] and established by Kojima [2]. Our recent experiments on this interesting magnetically driven superflow show a peculiar spin relaxation that is dependent on temperature and magnetic fields [3]. The results can be interpreted in terms of intrinsic spin relaxation based on Leggett and Takagi theory[4] and the predicted presence of small but increasing presence of minority spin pair condensate in A_1 phase [5].

In these measurements, we recognized a spin pumping effect and found a new method to derive the spin relaxation time in the A_1 phase. A sample cell has a large reservoir that is connected to a small detector chamber through a super leak made of two channels of width 20 μm. A flexible Myler

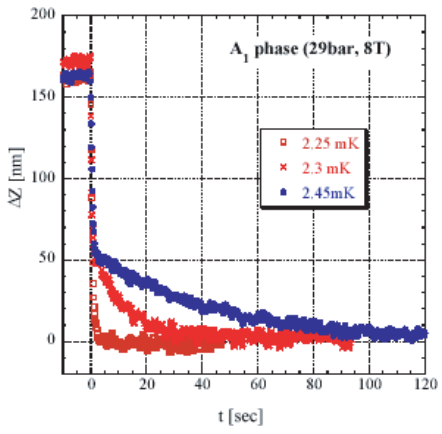

Fig. 1. Membrane's displacement corresponding to the pressure change in the A_1 phase at 29 bars and 8T.

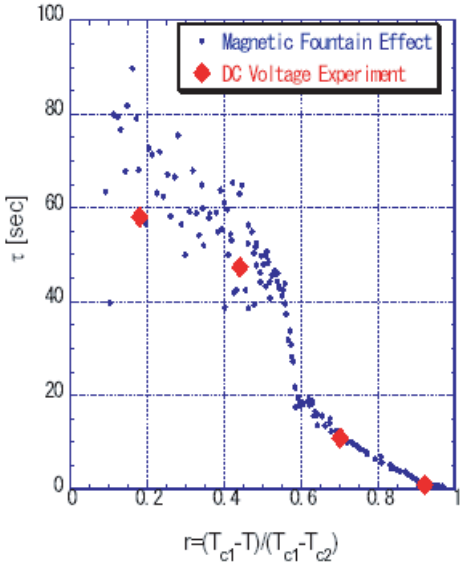

Fig. 2. Nominal spin relaxation time derived from mechanical and magnetic effects at 29 bars and 8T as a function of reduced temperature.

membrane dividing the two chambers forms a capacitance with a fixed electrode. It works as a very sensitive differential pressure sensor and also as a pump to produce a polarized spin flow into the detector chamber. A pulsed large DC voltage (about 30 V) on the capacitance sensor induces a simultaneous mass and spin superfluid flow into the small chamber (spin pump). After thermal equilibration, release of the DC voltage causes a sudden pressure drop followed by a slow relaxation (Fig.1). The sudden drop (ΔP) is a consequence of reversed superfluid flow through the superleak. It is compensated by the produced spin density difference (ΔS). The observed decay times during the slow relaxation are shown in Fig 2. They are in good agreement with the spin relaxation times obtained in the magnetic fountain effect. These observations support our interpretation that the observed slow relaxation stems from spin relaxation.

References
[1] M. Liu, Phys. Rev. Lett. **43**, 1740 (1979).
[2] R. Ruel and H. Kojima, Phys. Rev. B **28**, 6582 (1983).
[3] A. Yamaguchi, S. Kobayashi, H. Ishimoto, and H. Kojima, Nature **444**, 909 (2006).
[4] A. J. Leggett and S. Takagi, Ann. Phys. **106**, 79 (1977).
[5] H. Monien and L. Tewordt, J. Low Temp. Phys. **60**, 323 (1985).

Authors
A. Yamaguchi, S. Kobayashi, H. Ishimoto, and H. Kojima[a]
[a]Serin Physics laboratory, Rutgers University

Three-Dimensional Picture of the Interlayer Magnetoresistance of Quasi-One-Dimensional Layered Conductors

W. Kang and T. Osada

We have experimentally investigated the interlayer magnetoresistance of the representative quasi-one-dimensional (Q1D) layered organic conductor, $(TMTSF)_2PF_6$, over the full range of magnetic field orientations in three dimensions. We have also compared the obtained experimental results with existing semiclassical and quantum theories [1].

Figure 1(a) shows the stereographic plot of interlayer conductivity measured in $(TMTSF)_2PF_6$. The *x*-axis and *z*-axis correspond to the crystalline 1D (***a***-) axis and the

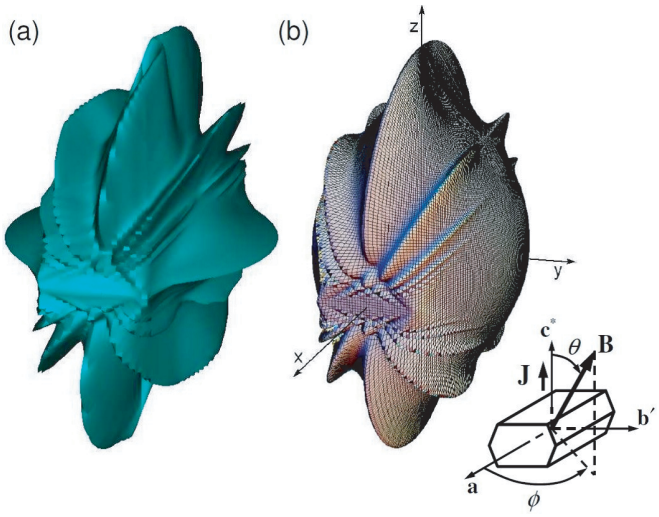

Fig. 1. Dependence of interlayer conductivity of Q1D conductors on magnetic field orientations. The distance and the direction from the origin indicate the logarithm of interlayer conductivity and the field orientation, respectively. (a) experiment in $(TMTSF)_2PF_6$. (b) calculation using analytic formula.

stacking (***c****-) axis, respectively. In the figure, the distance and the direction from the origin indicate the logarithm of interlayer conductivity and the field orientation, respectively. Fig.1(a) contains all of the angular effects known in Q1D conductors, that is, the Lebed resonance, the Danner-Kang-Chaikin oscillations, the third angular effect, and the Lee-Naughton oscillations. Although they have been discussed separately so far, the present results show that they are closely related one another in intermediate field orientations. We can see that the most fundamental effect is the Lebed magic angle resonance which looks like fins, and other effects result from the amplitude modulation of the Lebed resonance.

Figure 1(b) shows the stereographic plot of interlayer conductivity calculated for Q1D conductors based of analytic semiclassical theory, which corresponds to the lowest order contribution of interlayer coupling in the quantum theory. We can see that most of observed features are well explained by the existing theories. However, there is a critical discrepancy between experiment and theory, that is, the appearance of the horizontal fin in Fig.1(a). Experimentally, the interlayer conductivity shows remarkable enhancement under magnetic fields parallel to the conducting plane (*x*-*y* plane or crystalline ***a***-***b'*** plane). This is an anomalous magnetotransport behavior since the parallel field gives the Lorentz force most effectively.

Figure 2 shows the top view of Fig.1(a). We can see that the edge of the horizontal fin forms almost an perfect circle

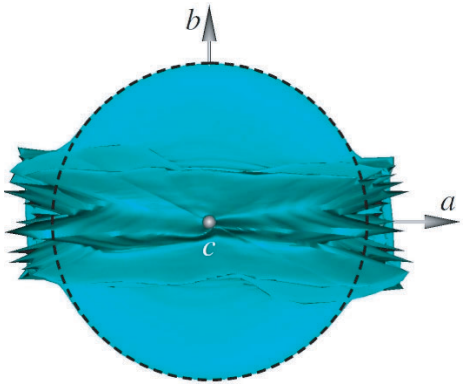

Fig. 2. Top view of Fig.1(a). The edge of the horizontal fin shows in-plane isotropy as shown by broken circle except near the ***a***-axis.

except near the 1D axis (crystalline ***a***-axis). It means that the in-plane conductance enhancement depends not on the in-plane field component but only on the normal field component B_z. This fact suggests that the in-plane conductance enhancement relates to some transport nature of 2D conducting planes.

According to the confinement theory proposed by Strong, Clark, and Anderson [2], the in-plane magnetic field decouples the multilayer to independent 2D layers, where interlayer conductivity obeys a scaling low depending only on B_z. Although the observed in-plane conductivity enhancement seem to be explained by the confinement theory, further experimental confirmation would be necessary.

References

[1] W. Kang, T. Osada, Y. J. Jo, and H. Kang, Phys. Rev. Lett. **99** (2007) to be published.

[2] S. P. Strong, D. G. Clarke, and P. W. Anderson, Phys. Rev. Lett. **73**, 1007 (1994).

Authors

W. Kang, Y. J. Jo, H. Kang, E. Ohmichi, K. Uchida, T. Konoike, and T. Osada

Discovery of the Most Stable Metallic Phase in Purely *d*-Electronic Conductors Based on the Transition-Metal Complex

K. Otsubo, H. Kitagawa, and Y. Uwatoko

Recent years, a halogen-bridged mixed-valence binuclear-metal complex, the so-called MMX-Chain, has been attracted significant attention owing to a variety of structural and physical properties derived from 1-D *d*-electron system [1]. The title complex, $Pt_2(dtp)_4I$ (dtp = $C_2H_5CS_2^-$) is a special case among MMX-Chain complexes, because it exhibits high electrical conductivity (~ 5 S cm^{-1}) and a metal-insulator transition at 205 K at ambient pressure indicating that its electronic states changes depending on temperature [2]. In this study, our attention focused on the novel electronic state of $Pt_2(dtp)_4I$ in the high pressure region, because an application of high pressure enables to control various physical parameters successively, such as electron-transfer-integral (t), lattice constant, electron-lattice interaction (S), and so on. To clarify the electrical transport property and electronic states of $Pt_2(dtp)_4I$ under high pressure, electrical resistivity measurement was performed using a cubic-anvil-press system. Here, we report that $Pt_2(dtp)_4I$ shows the most stable metallic phase in the 1-D d-electronic metal-complex-based system, and furthermore, we demonstrate a novel pressure-induced metal-insulator transition at 3.0 GPa.

Figure 1 (a) shows the pressure dependence of the electrical resistivity of $Pt_2(dtp)_4I$ along the b axis (// 1-D chain) at 298 K. As the pressure is increased, the electrical resistivity decreased rapidly, but a sharp transition at 3.0 GPa and a gradual decrease up to 8.0 GPa were observed. Temperature dependences of the electrical resistivity at 0, 2.2, 4.0, and 8.0 GPa are shown in Fig. 1 (b). At ambient pressure, the metal-insulator transition was observed at 205 K. Under 2.2 GPa, the metallic conduction was stabilized by pressure, metal-insulator transition temperature ($T_{M\text{-}I}$) was lowered down to 70 K. As is well known, the first 1-D molecular conductor $K_2Pt(CN)_4Br_{0.3}\cdot nH_2O$ (KCP(Br)) had so far held the lowest $T_{M\text{-}I}$ (= 210 K under 3.2 GPa) [3].

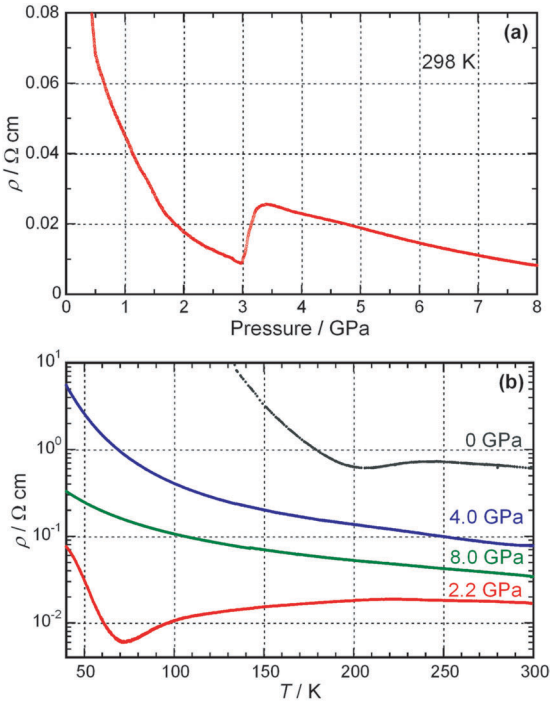

Fig. 1. (a) Pressure dependence of the electrical resistivity at 298 K. (b) Temperature dependences of the electrical resistivity under 0, 2.2, 4.0, and 8.0 GPa.

However, our result ($T_{M\text{-}I}$ = 70 K) is lower by 140 K and 1-D metallic phase of $Pt_2(dtp)_4I$ is much more stabilized. Thus, we demonstrated that $Pt_2(dtp)_4I$ is the most stable metal in 1-D purely *d*-electronic conductors based on the transition-metal complexes. On the other hand, the electrical transport behavior changed to be narrow gap semiconductor in the whole temperature region above 3.0 GPa. These results indicate that the resistivity jump at 3.0 GPa is due to a pressure-induced metal-insulator transition.

To clarify the origin of the pressure-induced metal-insulator transition, X-ray oscillation photographs were taken under high-pressure using a diamond-anvil-cell at KEK-PF BL-1B. Any diffuse scatterings or superlattice reflections at $k = n + 0.5$ (n : integer) originating from 2-fold periodic charge ordering, such as charge-density-wave (CDW : ·····Pt^{2+}-Pt^{2+}·····I–Pt^{3+}-Pt^{3+}–I–) or alternate-charge-polarization (ACP : ·····Pt^{2+}-Pt^{3+}–I–Pt^{3+}-Pt^{2+}·····I·····) states were not observed above 0.5 GPa at room temperature, suggesting that the electronic state above 0.5 GPa is not CDW or ACP but averaged-valence (AV : –$Pt^{2.5+}$-$Pt^{2.5+}$–I–$Pt^{2.5+}$-$Pt^{2.5+}$–I–) or charge-polarization (CP : ·····Pt^{2+}-Pt^{3+}–I·····Pt^{2+}-Pt^{3+}–I–) states. Pressure dependences of the lattice constant b and unit cell volume V at room temperature are shown in Fig. 2. These parameters decreased monotonically with applying pressure, but the discontinuous jump was observed at 3.0 GPa. These results indicate that the pressure-induced metal-

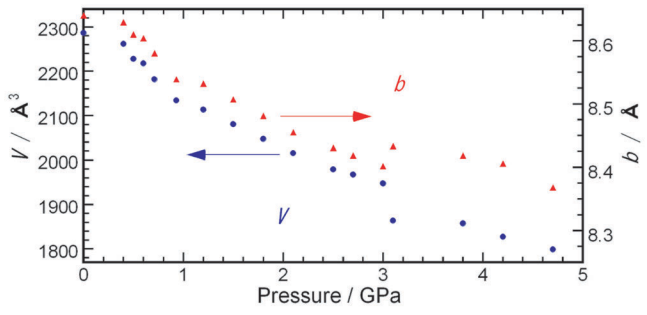

Fig. 2. Pressure dependences of the lattice parameter b (red) and unit cell volume V (blue).

insulator transition at 3.0 GPa is attributable to a first-order structural phase transition with elongation of *b*-axis (// chain) resulting in a lowering of the electron transfer integral (*t*) [4]. Our present results of Raman sprectra under high pressure supported this structural phase transition at 3.0 GPa.

References

[1] C. Bellito, A. Flamini, L. Gastaldi, and L. Scaramuzza, Inorg. Chem. **22**, 444 (1983).
[2] M. Mitsumi, T. Murase, H. Kishida, T. Yoshinari, Y. Ozawa, K. Toriumi, T. Sonoyama, H. Kitagawa, and T. Mitani, J. Am. Chem. Soc. **123**, 11179 (2001).
[3] M. Thielemans, R. Deltour, D. Jerome, and R. Cooper, R. J. Solid State Commun. **19**, 21 (1976).
[4] K. Otsubo, A. Kobayashi, H. Kitagawa, M. Hedo, Y. Uwatoko, H. Sagayama, Y. Wakabayashi, and H. Sawa, J. Am. Chem. Soc. **128**, 8140 (2006).

Authors

K. Otsubo[a], A. Kobayashi[a], H. Kitagawa[a], M. Hedo, Y. Uwatoko, H. Sagayama[b], Y. Wakabayashi[b], and H. Sawa[b]

[a]Department of Chemistry, Faculty of Science, Kyushu University

[b]Photon Factory, Institute of Materials Structure Science, High-Energy Accelerator Research Organization

New Ordered State in the Strongly Correlated Oxide $BaIrO_3$

T. Nakano and Y. Uwatoko

Discovery of a new ordered state is one of the most interesting topic in condensed matter physics. $BaIrO_3$ is a promising candidate in which a new ordered state may be realized. The crystal structure of $BaIrO_3$ is monoclinic with a zigzag chain of Ir_3O_{12} trimers along the *c* axis [1] as shown in the inset of Fig 1. Each trimer shares the corner with a neighboring trimer, and forms a corrugated honeycomb network along the *ab* plane. $BaIrO_3$ shows weak ferromagnetism with small magnetic moment of 0.04 μ_B/Ir below T_c = 180 K [2-4] and a gap-type order characterized by a hump-type resistivity [3, 4], a hum-type Seebeck coefficient [4, 5] and a gap-like optical spectrum [6] below T_c. Fermi surface nesting is predicted by the band calculation [7], and a charge-density-wave (CDW) state was proposed as an origin of the gap-type ordered state [3]. However, direct evidence for CDW, that is, satellite reflections or soft phonons is not yet observed at present. To clarify the nature of the 180-K transition, we measured the pressure dependence of the resistivity.

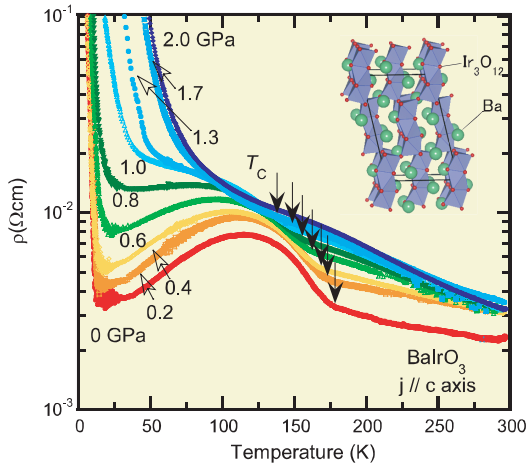

Fig. 1. Pressure dependence of the resistivity of a single-crystal sample of $BaIrO_3$ along to the *c* axis. Inset: Schematic crystal structure of $BaIrO_3$.

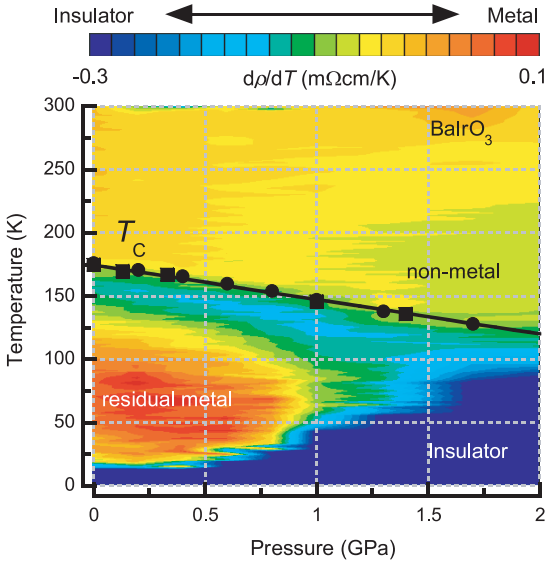

Fig. 2. Tow-dimensional color plot of dρ/dT of $BaIrO_3$ on the temperature-pressure phase diagram.

Figure 1 displays the resistivity ρ of $BaIrO_3$ under pressure along the *c* axis. At ambient pressure, the resistivity gradually increases with decreasing temperature from 300 K down to T_c, and shows a hump-type anomaly at T_c. With further decreasing temperature, it shows a broad maximum at around 120 K, and decreases down to 20 K with metallic temperature dependence (dρ/dT>0). Below 20 K, the resistivity suddenly increases again. By applying pressure, the resistivity is dramatically increased, and the metallic conduction below T_c disappears above 1 GPa. This is quite unconventional pressure dependence. T_c shifts to lower temperature with increasing pressure. Pressure dependence of T_c (dT_c/dP) evaluated to be –29 K/GPa is relatively large, suggesting that the electronic states are coupled with the lattice. However, if the ground state were CDW, the normal state above T_c should be metallic. This is seriously incompatible to the fact that pressure makes the system more insulative in spite of $dT_c/dP < 0$.

Figure 2 displays the *T*-*P* phase diagram by using a two-dimensional color plot of dρ/dT and $T_c(P)$. The boundary between the yellow and blue colors is clearly illustrated below 1 GPa, and the metallic conduction is highlighted by the red color. Above 1 GPa, the phase boundary is somewhat smeared, and the insulating region below T_c seems to merge with non-metal region above T_c.

Instead of the CDW scenario, we propose an alternative model for the 180-K transition. Let us consider the electronic states of a Ir_3O_{12} trimer by neglecting the inter-trimer hopping. For the trigonally distorted IrO_6 octahedron, a_{1g} level is half filled by 5d electrons of Ir^{4+}. Three a_{1g} orbitals of each trimer would then compose the bonding(B), non-bonding(NB) and anti bonding(AB) states. When hybridization in the inter-trimer is sufficiently small, $BaIrO_3$ can be regarded as a half-filled system, in which one *5d* electron occupies the NB state with the other two electrons occupying the bonding state on each trimer. Thus the insulating state above T_c can be regarded as a Mott insulator. On the other hand, two inequivalent trimers due to the monoclinic distortion cause a finite energy difference ΔE between the NB states. ΔE would increase with decreasing temperature, because the $BaIrO_3$ shows negative thermal expansion along the *c* axis(not shown). At a certain temperature, charge transfer can occur from the higher to lower NB state when ΔE exceeds the intra-trimer Coulomb repulsion. In this

context, the charge-transferred state below T_c may be regarded as a band insulator. We believe that this is the origin of the 180-K transition of $BaIrO_3$.

References

[1] T. Siegrist and B. L. Chamberland, J. Less-Common Met. **170**, 93 (1991).
[2] R. Lindsay, W. Strange, B. L. Chamberland, and R. O. Moyer, Jr, Solid State Commun. **86**, 759 (1993).
[3] G. Cao, J. E. Crow, R. P. Guertin, P. F. Henning, C. C. Homes, M. Strongin, D. N. Basov, and E. Lochner, Solid State Commun. **113**, 657 (2000).
[4] T. Nakano and I. Terasaki, Phys. Rev. B **73**, 195106 (2006).
[5] N. S. Kini, A. Bentien, S. Ramakrishnan, and C. Geibel, Physca B **359-369**, 1264 (2005).
[6] K. Maiti, R. S. Singh, V. R. R. Medicherla, S. Rayaprol, and E. V. Sampathkumaran, Phys. Rev. Lett. **95**, 016404 (2005).
[7] M. -H. Whangbo and H. -J. Koo, Solid State Commun. **118**, 491 (2001).

Authors

T. Nakano[a,b], I. Terasaki[a,b], M. Hedo, and Y. Uwatoko
[a]Waseda University
[b]CREST/JST

Physical Properties and Pressure effect on T_N in $SmMIn_5$ (M=Co, Rh, Ir)

Y. Inada and Y. Uwatoko

$SmMIn_5$ (M = Co, Rh, Ir) crystallizes in the tetragonal $HoCoGa_5$-type structure. This type of crystal structure is known as a tetragonal variant of the $AuCu_3$ cubic crystal structure, and in which new superconductors were discovered [1, 2]. $CeMIn_5$ (M = Co, Rh, Ir) compounds exhibit a variety of interesting properties such as non-*s*-wave-superconductivity, a first-order transition near the upper critical field, heavy-fermion behavior, pressure-induced superconductivity, etc. [3, 4]. Recently, superconductivity in $PuCoGa_5$ and $PuRhGa_5$ was discovered, and they are known as heavy-fermion "high T_c" superconductors [2,5]. In the exotic heavy fermion superconductors, Cooper pairs are expected formed

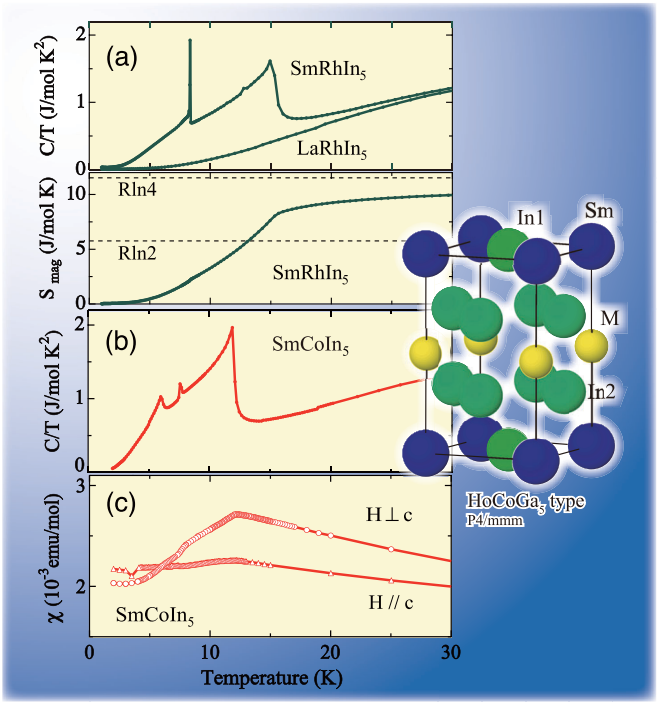

Fig.1. (a) Specific heat divided by temperature (C/T) and corresponding magnetic entropy as a function of temperature for $SmRhIn_5$, (b) C/T vs T for $SmCoIn_5$, and (c) static magnetic susceptibility χ of $SmCoIn_5$.

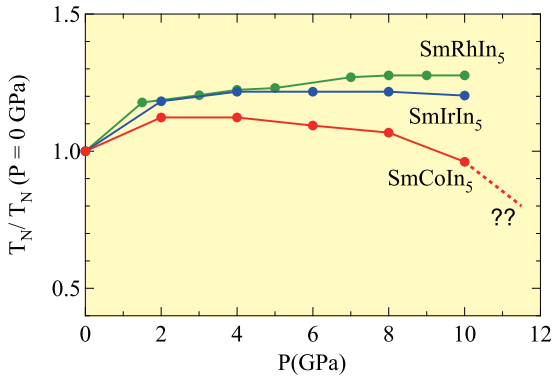

Fig. 2. Pressure dependence of the ratio of T_N to T_N at 0 GPa on $SmMIn_5$.

by the exchange of magnetic spin fluctuations, in which *f*-electrons are not simply localized and they play an important role. A large specific heat coefficient and low antiferromagnetic ordering temperatures are features of the exotic heavy-fermion superconductors.

Pu has valence states of Pu^{3+} ($5f^5$), Pu^{4+} ($5f^4$), Pu^{5+}, Pu^{6+} in Pu based compounds, while it is known that Sm has Sm^{2+} ($4f^6$), Sm^{3+} ($4f^5$). Sm^{3+} ($4f^5$) and Pu^{3+} ($5f^5$) ions have the same J=5/2 multiplet, and show the local moment behavior, *i.e.*, obey a Curie-Weiss law. It is interesting that it depends on the particular crystal structure whether Sm compounds show exotic behavior or not. It is interesting to compare $SmMIn_5$ and heavy fermion "high T_c" superconductors of $PuCoGa_5$ and $PuRhGa_5$.

We have succeeded in growing single crystals of $SmMIn_5$ (M= Co, Rh, Ir) by the flux method [6]. The physical properties of single crystals of $SmRhIn_5$ and $SmIrIn_5$ have already been reported [7], but there was no report on single-crystalline $SmCoIn_5$ before our works.

Figure 1(a) shows the specific heat divided by temperature and the corresponding magnetic entropy below 30 K, for $SmRhIn_5$ and $LaRhIn_5$. The non-magnetic contribution of $LaRhIn_5$ has been subtracted from the specific heat of $SmRhIn_5$ to calculate the magnetic entropy. Two clear peaks were observed, of which the upper one corresponds to the antiferromagnetic order. The upper transition temperature T_N is 15.0 K. The lower transition temperature is 8.3 K. The magnetic entropy is about 75% of Rln4 at T_N. This is similar to the case of $SmSn_3$ with $AuCu_3$ cubic crystal structure [8]. The ground-state level of $SmSn_3$ is a Γ_8 [8], however, Γ_8 quartet splits into two doublets in the tetragonal crystal structure, leading to three doublets. It is probable that there are two adjacent doublet levels in $SmRhIn_5$. $SmRhIn_5$ shows the localized *f* electron nature.

Figure 1(b) shows the specific heat divided by temperature versus temperature for $SmCoIn_5$, and Fig. 1(c) the static magnetic susceptibility measured in an applied field of 0.1 T for the field along the *c* axis (triangles) and perpendicular to the *c* axis (circles) below 30K. The magnetic susceptibility shows anisotropic behavior similar to $SmRhIn_5$. Three anomalies are observed both in the temperature dependence of C/T and χ. The temperatures of these anomalies are 6 K, 7.6 K and 11.9 K. The Neel temperature of 11.9 K is the lowest value found in $SmMIn_5$ compounds. It is expected that $SmCoIn_5$ is closer to the delocalized state than $SmRhIn_5$ and $SmIrIn_5$. However, the value of C/T at 2 K in $SmCoIn_5$ is 53mJ/molK^2 which is not a large value compared to $PuCoGa_5$ or $PuRhGa_5$. Therefore, it may be concluded that the 4*f* electrons in $SmCoIn_5$ are more localized than 5*f* electrons in $PuCoGa_5$.

In order to track the pressure evolution of the value of T_N, we have measured the electrical resistivity on single crystals of $SmMIn_5$ using a cubic anvil pressure cell at temperature 2-300 K under high pressure from 2 to 10 GPa. Figure 2 shows the pressure dependence of the ratio of T_N to that at ambient pressure. The T_N at ambient pressure is 15.0 and 14.9 and 11.9 K for $SmRhIn_5$, $SmIrIn_5$ and $SmCoIn_5$, respectively. This result indicates there is a tendency for T_N to clearly decrease with lower T_N at ambient pressure. The extent of delocalization probably becomes larger in order of $SmCoIn_5$ > $SmIrIn_5$ > $SmRhIn_5$. The similar tendency was observed in $CeMIn_5$. The *d* band levels in M may be concerned with delocalization of 4*f* electrons. The pressure evolution of T_N above 10 GPa is interesting, especially in $SmCoIn_5$. What kind of state of 4*f* electrons will realize at higher pressure range in $SmCoIn_5$?

References

[1] J. D. Thompson *et al.*, J. Magn. Magn. Mater. **226**, 5 (2001).
[2] J. L. Sarrao *et al.*, Nature **420**, 297 (2002).
[3] A. Bianchi *et al.*, Phys. Rev. Lett. **91**, 187004 (2003).
[4] H. Hegger *et al.*, Phys. Rev. Lett. **84**, 4986 (2000).
[5] F. Wastin *et al.*, J. Phys. Condens. Matter **15**, S2279 (2003) .
[6] Y. Inada *et al.*, Physica B **378-380**, 421 (2006).
[7] P. G. Pagliuso *et al.*, Phys. Rev. B **63**, 054426 (2001).
[8] M. Kasaya *et al.*, J. Magn. Magn. Mater. **52**, 289 (1985).

Authors

Y. Inada[a], T. Sadamasa[a], M. Koeda, M. Hedo, T. Fujiwara, and Y. Uwatoko

[a]Department of Science Education, Faculty of Education, Okayama University

New Models of Polymer Crystallization under Shear: Shish-Kebab Structure Revisited

Shibayama Group

In the rich and long-standing literature on the flow-induced formation of oriented precursors to polymer crystallization, it is often asserted that the longest, most extended chains are the dominant molecular species in the "shish" of the "shish-kebab" formation [1]. We performed a critical examination of this widely held view, using deuterium labeling to distinguish different chain lengths within an overall distribution. Small-angle neutron-scattering (SANS) patterns of the differently labeled materials showed that long chains are not overrepresented in the shish relative to their concentration in the material as a whole. We observed that the longest chains play a catalytic role, recruiting other chains adjacent to them into formation of the shish.

Three model isotactic polypropylene (iPP) resins with well-matched overall molar mass distributions-but different chain lengths labeled with deuterium-were prepared by blending hydrogenated and deuterated polymers. These three model resins contained labeled chains of 13 wt% in the shortest third (M_w = 41 kg/mol), the middle third (M_w = 197 kg/mol), or the longest third (M_w = 1781 kg/mol) of the overall distribution, denoted Short-D, Medium-D, and Long-D, respectively. Here, M_w is the molecular weight of the labeled iPPs. Each of the deuterium-labeled resins was subjected to identical flow at 180°C and thermal history to form specimens that had a skin-core morphology. The transient response during and after flow, as well as final morphology, was consistent for the three samples. During the shear pulse, all three materials showed similar birefringence traces, characteristic of formation of oriented precursors.

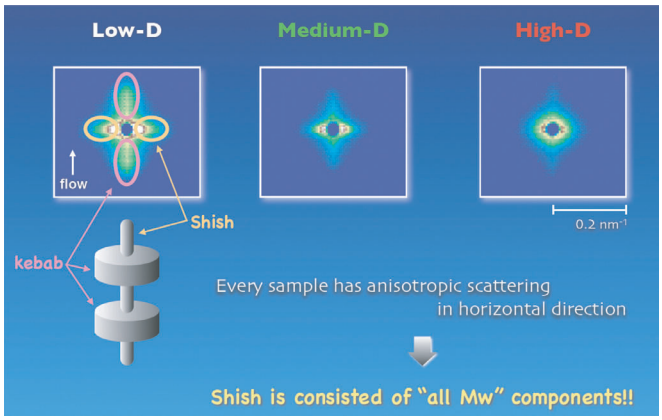

Fig. 1. SANS patterns of iPPs blended with Low-D, Medium-D, and High-D, and a model of shish-kebab structure showing the relationship.

Very different SANS patterns were observed as a function of the length of the labeled chains (Fig. 1) [2]. Parent lamellar stacks were clearly evident in all three samples as the lobes of intensity in the meridional direction; strong equatorial scattering was evident near the beamstop. The sample containing deuterated short chains exhibited much stronger scattering than those with labeled medium or long chains. In Short-D, the deuterium label became concentrated in the lamellar crystallites. Because their coil dimensions are smaller than the long spacing, the short chains rarely form tie chains between neighboring lamellae, so few of their segments become trapped in the interlamellar region. Thus, the short chains abandon the interlamellar region, but medium and long chains are trapped there, both because they cannot add to the growth front as quickly as it passes by and because they are more likely to be frustrated by attaching to multiple stacked lamellae. Therefore, the scattering from the lamellar stacks in Medium-D and Long-D is much weaker and arises from a relative excess of deuterium in the noncrystalline interlamellar material. The elevated orientation created near the shish causes rapid ordering. Direct measurement of chains of different lengths partitioning into the shish shows that the fraction of long-chain segments within the shish matches their composition in the melt as a whole. This indicates that the long chains recruit neighboring chains to join them in forming the shish (Fig. 2) [2, 3].

References

[1] Z. Bashir, J. A. Odell, and A. Keller, J. Mater. Sci. **21**, 3993 (1986).
[2] S. Kimata, T. Sakurai, Y. Nozue, T. Kasahara, N. Yamaguchi, T. Karino, M. Shibayama, and J. A. Kornfield, Science **316**, 1014 (2007).
[3] M. Seki, D. W. Thurman, J. P. Oberhauser, and J. A. Kornfield, Macromolecules **35**, 2583 (2002).

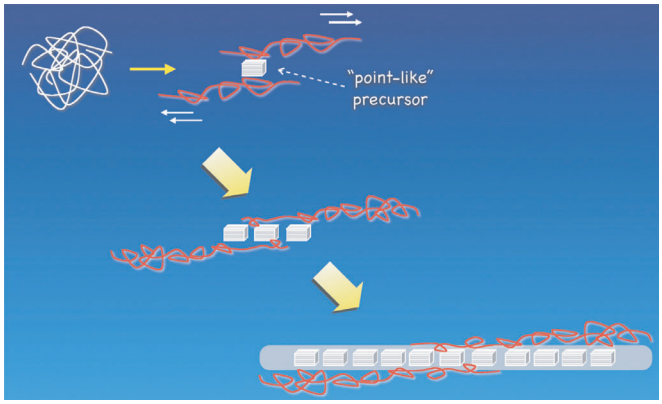

Fig. 2. Mechanism of shish-kebab formation.

Authors
S. Kimata[a,b], T. Sakurai[a], Y. Nozue[a], T. Kasahara[a], N. Yamaguchi[a], T. Karino, M. Shibayama, and J. A. Kornfield[b]
[a]Petrochemicals Research Laboratory, Sumitomo Chemical
[b]Division of Chemistry and Chemical Engineering, California Institute of Technology

Epitaxial A-site Ordered Perovskite Manganite $SmBaMn_2O_6$ Thin Film on $SrTiO_3(001)$

T. Nakajima and Y. Ueda

Perovskite manganites have been intensively studied about their huge MR effect, the so-called colossal magnetoresistance (CMR) effect. In perovskite manganite thin films that show the CMR effect, the light-induced insulator-metal transition has also been realized in the CMR manganites by Takubo *et al.* [1]. Because of these properties, the perovskite manganites show promise for applications such as electronic switching devices that use a magnetically or optically induced phase change. However, CMR manganites such as $La_{1-x}Ca_xMnO_3$ have a disadvantage for the application: namely, the CMR is observed far below room temperature. Therefore, the development of new materials that exhibit CMR near room temperature is desirable. Recently, we synthesized A-site ordered manganites $RBaMn_2O_6$, and discovered that La-doped $SmBaMn_2O_6$ exhibits 1000% CMR under 9 T at 300 K [2]. However, the thin films of A-site ordered perovskite manganites have not been prepared so far by conventional film-forming methods, while the fabrication of films is essential for the practical applications. Therefore, we have investigated the fabrication of A-site ordered manganite thin films using a new process, an excimer laser assisted metal organic deposition (ELAMOD) process. An A-site ordered perovskite manganite $SmBaMn_2O_{6-\delta}$ ($\delta \cong 0.5$) film was fabricated by means of the ELAMOD, and epitaxially grown on a $SrTiO_3(001)$ substrate. The $SmBaMn_2O_{6-\delta}$ film was crystallized in [010]- and [001]-oriented domains that were confirmed by X-ray diffraction and cross-section transmittance electron microscopy (TEM) as shown in Fig. 1. The A-site ordered structure formed at 500 °C under KrF laser irradiation at a laser fluence of 140 mJ/cm^2 for 60 min in an Ar flow, whereas disordered A-site cations formed under laser irradiation at fluences less than 120 mJ/cm^2 and/or in an oxygen atmosphere. A $SmBaMn_2O_6$ film was obtained by oxygen annealing of the as-prepared $SmBaMn_2O_{6-\delta}$ film at 500 °C for 3 h. The electrical resistivity for the $SmBaMn_2O_6$ film on $SrTiO_3(001)$ show insulating behavior without a first-order charge/orbital order (CO) transition caused by constraint of lattice change associated with the CO due to the undeformable substrate lattice. The ELAMOD process is expected to serve as a new key technique for the fabrication of A-site ordered perovskite manganite thin films.

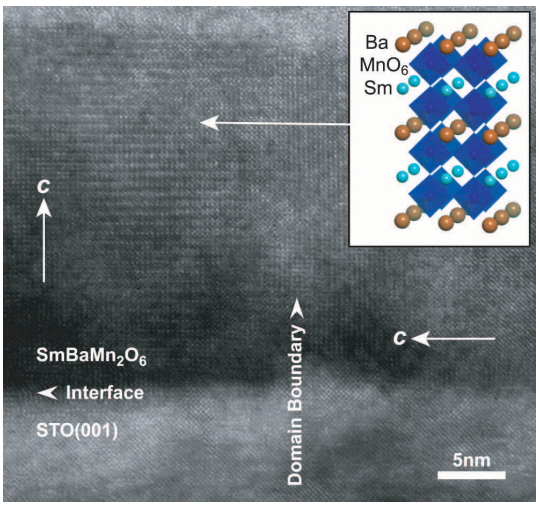

Fig. 1. Cross-sectional TEM image of the $SmBaMn_2O_6$ film on $SrTiO_3(001)$.

References
[1] N. Takubo, Y. Ogimoto, M. Nakamura, H. Tamaru, M. Izumi, and K. Miyano, Phys. Rev. Lett. **95** 017404 (2005).
[2] T. Nakajima and Y. Ueda, J. Appl. Phys. **98** 046108 (2005).

Authors
T. Nakajima[a], T. Tsuchiya[a], M. Ichihara, Y. Ueda, and T. Kumagai[a]
[a]National Institute of Advanced Industrial Science and Technology

Electronic Structure of β-$FeSi_2$

H. Udono, K. Takarabe, and H. Tajima

Semiconducting iron disilicide, β-$FeSi_2$, is increasingly attracting attention as a suitable material for use in Si-based optoelectronics, because β-$FeSi_2$ has a band gap in the near infrared (NIR) region and a very high refractive index (5-6), and its film is epitaxially grown on Si substrate using a conventional Si-ULSI process. Recent reports on the 1.56 - 1.6 μm light emitting diodes and high index-contrast photonic crystal devices using β-$FeSi_2$/Si have dramatically remotivated the interest in β-$FeSi_2$ [1]. However, the luminescence mechanism and the electronic structure have not been clarified, yet. The band gap nature of bulk β-$FeSi_2$ is indirect and its gap energy is expected to be around 0.7eV at 300K [2, 3]. Thus, we have investigated the electronic structure using the band calculation based on the first-principles method and polarized optical reflection (PR) measurements on single crystalline β-$FeSi_2$.

The calculated band structure is shown in Fig. 1(a). The band structure of β-$FeSi_2$ was characterized by an indirect transition of 0.67eV between the valence band maximum (VBM) at the *Y* point and the conduction band minimum

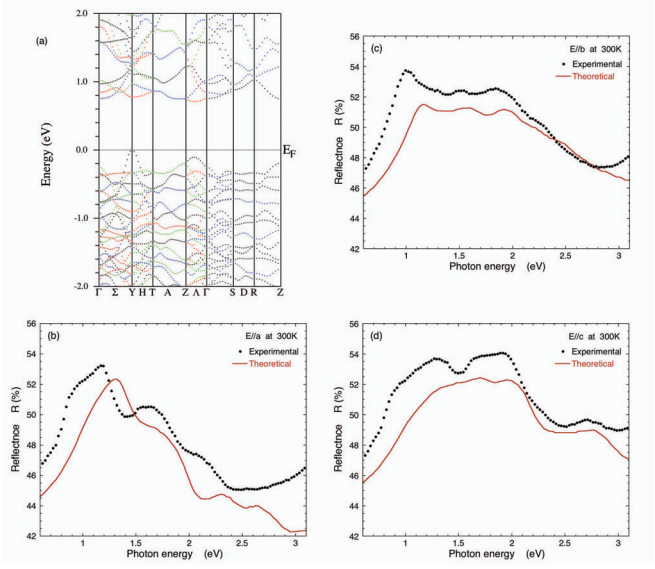

Fig. 1. (a) Band structure of β-$FeSi_2$ along high symmetry axes. The valence-band maximum at the *Y* point is taken as the reference energy. PR spectrums of β-$FeSi_2$ single crystal for (b) E//a, (c) E//b, and (d) E//c light polarization. The solid lines are the theoretical spectrums.

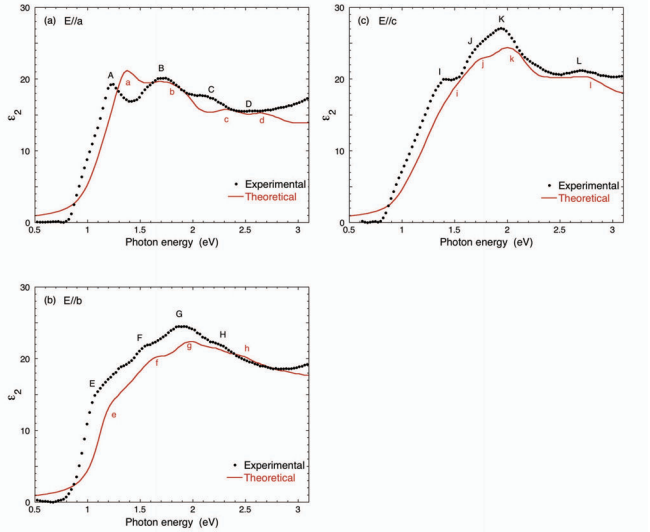

Fig. 2. Imaginary parts (ε_2) of the dielectric function of β-$FeSi_2$ single crystal for (a) E//a, (b) E//b, and (c) E//c light polarization. The solid lines are the theoretical spectrums. A-L and a-l denote the peaks or shoulders in the experimental and theoretical spectrum, respectively.

(CBM) situated along the *G*-*Z* (*L*) direction. The first direct transition gap was 0.73eV at the *Y* point. The next direct band gap was 0.81eV at *L* point. Figure 1(b)-1(d) show a comparison of the PR spectrums for the experimental and theoretical results. The PR spectrums for E//a, E//b and E//c reveal that the anisotropy of the reflectance depending on the light polarization. Features of each experimental spectrum are comparable to the theoretical calculations [4].

Figure 2 shows a comparison of the imaginary part of the dielectric function, ε_2, for the experimental and theoretical data. The spectrums for E//a, E//b and E//c had characteristically four peaks or shoulders in each spectrum as denoted A-L for experimental and a-l for theoretical data, respectively. When the theoretical spectrums are shifted 0.8- 0.14 eV to the lower energy, the transition energies at the peaks or shoulders in the experimental spectrums corresponds well to those in the theoretical ones, *e.g.*, A-D, E-H and I-L correspond to a-d, e-h and i-l, respectively. Furthermore, relative intensity of each peak or shoulder in both experimental and theoretical spectrums (A-L and a-l) agreed well in each other. These analyses of the spectrums indicate that the energy dependence of the dielectric function up to 3.1eV is well reproduced by the theoretical calculation using the FLAPW method based on the DFT and the dipole approximation.

We found that the optical properties (absorption and PR spectrum) of bulk β-$FeSi_2$ are well explained by the band calculation based on the first-principles method. However, there remain some unsolved problems. The value of direct gap energy at *Y*-*Y* in the electronic structure is under estimated about 0.21eV compared to the absorption experiments [3]. On the other hand, analysis of the PR spectrums suggests the over estimation of the calculated transition energy for the higher interband transitions. If we assumed that the temperature shift of the PR spectrum is about 0.04eV at 0K as observed in the absorption spectrum, the offset energy of about +0.1eV is derived. This value is not negligible compared to the experimental uncertainty. Therefore, the shift of the theoretical peak position to the higher energy as compared to the experimental one could suggest that some additional effects should be taken into account the theoretical calculation.

References
[1] T. Suemasu *et al.*, Jpn. J. Appl. Phys. **39** L1013 (2000).
[2] H. Udono, I. Kikuma, T. Okuno, Y. Masumoto, and H. Tajima, Appl. Phys. Lett. **85**, 1937 (2004).
[3] H. Udono, I. Kikuma, T. Okuno, Y. Masumoto, H. Tajima, and S. Komuro, Thin Solid Films **461**, 182 (2004).
[4] H. Udono, I. Kikuma, H. Tajima, and K. Takarabe, J. Mater. Sci., DOI 10.1007/s10854-007-9166-z (2007).

Authors
H. Udono[a] K. Takarabe[b] and H. Tajima
[a]College of Engineering, Ibaraki University
[b]Okayama University of Science

Giant Intrinsic Spin Hall Effect in Transition Metal Complexes [Sr_2RuO_4, Platinum]

H. Kontani, D. S. Hirashima, and J. Inoue

Recently, spin Hall effect (SHE) attracts great attention due to its fundamental interest and its potential application in spintronics. In 1954, Karplus and Luttinger showed that an electric field induces a spin-dependent transverse current in the presence of spin-orbit (SO) interaction. This mechanism causes the anomalous Hall effect in ferromagnetic metals, and the SHE in paramagnetic metals. Recent experiment [1] revealed that the spin Hall conductivity (SHC) obtained by a non-local measurement for Pt is 10^4 times larger than that in semiconductors. This fact devoted considerable attention to the SHE in transition metals.

To elucidate the origin of huge SHE in Pt, we focused attention to the significance of d-orbital degrees of freedom, and studied the SHC in several multiorbital tight-binding models [2, 3, 4]: Figure 1 shows a two-dimensional (d_{xz}, d_{yz})-orbital tight-binding model [2], which is a simplified model for Sr_2RuO_4 [3]. Here, $\pm t'$ represents the interorbital hopping integral between next nearest sites. Now, let us consider the motion of a down-spin electron along a triangle of half unit cell: An electron in the d_{xz}-orbital can transfer to d_{yz}-orbital and vise versa using the z-component of SO interaction $-\hbar\lambda l_z/2$ where $\langle\, xy \mid l_z \mid yz \,\rangle = -\langle\, yz \mid l_z \mid xz \,\rangle = i$. By combination of angular dependence of interorbital hopping and the SO interaction, a clockwise (anti-clockwise) motion along any triangle path with SO interaction causes the factor $+i$ ($-i$). This factor can be interpreted as the Aharonov-Bohm phase factor $\exp(2\pi i\phi/\phi_0)$ [$\phi_0 = hc/|e|$], where $\phi = \pm\phi_0/4$ represents the "effective magnetic flux" in the half unit cell. We revealed that the effective magnetic flux, which is inherent in multiorbital d-electron systems, causes huge SHE in various transition metals [2, 3, 4].

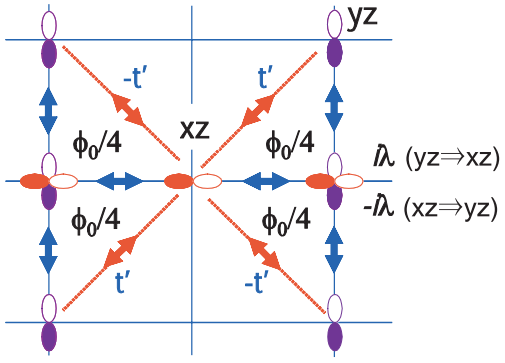

Fig. 1. Effective magnetic flux for down-electron in a (d_{xz},d_{yz})-orbital tight-binding model.

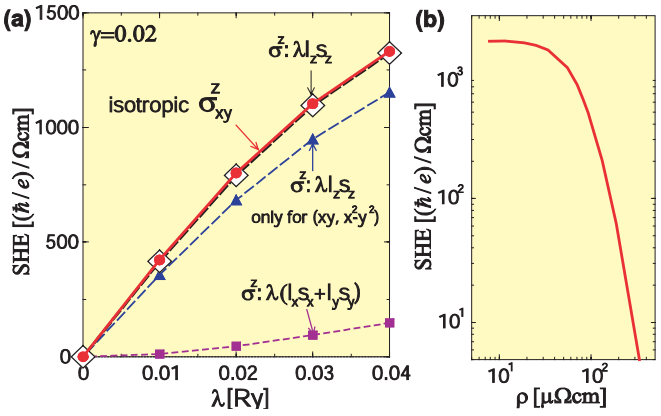

Fig. 2 .(a)λ-dependence of the SHC in Pt. γ represents the quasiparticle damping rate. (b) SHC as a function of resistivity ρ ($\propto \gamma$).

Here, we calculate the SHC based on the linear-response theory: Figure 2 (a) shows the SHC (σ^z_{xy}) in a (6*s*,6*p*,5*d*)-tight-binding model for Pt [3], as a function of the SO interaction λ. The value of λ for 5d-electrton in Pt is expected to 0.03 Ry. In this case SHC exceeds 1000$\hbar/e\Omega$cm, which is four times large that the experimental value in Pt at room temperature [1]. To clarify the origin of SHE in Pt, we study the SHC when the SO interaction is anisotropic: Whereas SHC for the XY-like SO interaction $\lambda(l_x s_x + l_y s_y)$ is very small, SHC for the Ising-like SO interaction $\lambda l_z s_z$ is as large as that in the isotropic case. Especially, matrix elements of $\lambda l_z s_z$ between (d_{xy}, $d_{x2\text{-}y2}$)-orbitals, both of which are composed of $l_z = \pm 2$ gives the dominant contribution to the SHC. Figure 2 (b) shows that the SHC is constant for $\rho << 30\,\mu\Omega$cm, whereas it decreases quickly for $\rho >> 30\,\mu\Omega$cm. This coherent-incoherent crossover behavior of the intrinsic SHC also appears in the anomalous Hall effect [2].

The present study strongly suggests that giant SHE due to the mechanism of "effective magnetic flux" is not restricted to Sr_2RuO_4 and platinum, but is ubiquitous in various *p*-, *d*-, *f*-electron systems with atomic orbital degrees of freedom.

References
[1] T. Kimura, Y. Otani, T. Sato, S. Takahashi, and S. Maekawa, Phys. Rev. Lett. **98**, 156601 (2007).
[2] H. Kontani, T. Tanaka, and K. Yamada, Phys. Rev. B **75**, 184416 (2007).
[3] H. Kontani, T. Tanaka, D. S. Hirashima, K. Yamada, and J. Inoue, cond-mat/ 0702447.
[4] H. Kontani, M. Naito, D. S. Hirashima, K. Yamada, and J. Inoue, arXiv:0705.3535.

Authors
H. Kontani[a], T. Tanaka[a], M. Naotio[a], D. S. Hirashima[a], K. Yamada[b], and J. Inoue[c]
[a]Department of Physics, Nagoya University
[b]Ritsumeikan University
[c]Department of Applied Physics, Nagoya University

1/3 Magnetization Plateau in S = 1/2 Quasi-Two-Dimensional Antiferromagnet $(CuBr)Sr_2Nb_3O_{10}$

H. Kageyama and K. Kindo

Historically, the study of geometrically frustration in spin systems has been centered on the triangle-based models such as triangular, kagomé and pyrochlore lattices. This is because they simply consist of single elements of NN interactions (J_1), and the abundance of experimental examples. On the other hand, frustration in square-based models that involve addition of 2NN (J_2) interactions is difficult to be realized because nature favors the dominance of the interactions for shorter bonds, resulting in the well-known (π, π) Néel ordered state.

Double-layered perovskites (Cu*X*)$LaNb_2O_7$ (*X* = Cl, Br), in which Cu^{2+} spins forms the *S* = 1/2 square lattice, have been found to show intriguing phenomena related to geometrical frustration. (CuBr)$LaNb_2O_7$ establishes a (π, 0) collinear AF order (CAF) at 32 K with a reduced moment ~ 0.6 μ_B, while (CuCl)$LaNb_2O_7$ has the spin-singlet ground state, with a gap of 2.3 meV in the spin excitation spectrum [1, 2]. (Cu*X*)$LaNb_2O_7$ belongs to the Dion-Jacobson series expressed as (Cu*X*)$A_{n-1}B_nO_{3n+1}$, where *A* is La^{3+}, Ca^{2+}, Na^{+}..., *B* is Nb^{5+}, Ta^{5+}, Ti^{4+}, *n* = 2, 3, 4.... The rich diversity of the family brings a crucial advantage over existing compounds, that is, a systematic control of the magnetic properties by varying parameters *A*, *B*, *X* and *n*. Particularly interesting is tuning *n*, by which one can control the two-dimensionality (2D).

Here, we newly synthesized a triple-layered perovskite $(CuBr)Sr_2Nb_3O_{10}$ from the ion-exchange reaction expressed as "$RbSr_2Nb_3O_{10} + CuBr_2 \rightarrow (CuBr)Sr_2Nb_3O_{10} + RbBr$" and measured magnetic properties [3]. Figure 1 shows the pulsed-field magnetizations divided by the saturated magnetization $M(H)/M_s$. The most prominent aspect is the appearance of a plateau corresponding to the 1/3 of the full magnetization, which was not found in the double-layered system. The plateau becomes obscured with increasing *T* and vanishes at 9 K. The 1/3 magnetization plateau has been theoretically predicted for various triangle-based lattices, as experimentally verified by, *e.g.*, Cs_2CuBr_4 and a copper complex. However, for commensurability reasons calculations of the square lattice predict plateaus such as 1/2 and 1/4. The present study thus calls for further attention to the frustrated square-lattice system.

References
[1] H. Kageyama, T. Kitano, N. Oba, M. Nishi, S. Nagai, K. Hirota, L. Viciu, J. B. Wiley, J. Yasuda, Y. Baba, Y. Ajiro, and K. Yoshimura, J. Phys. Soc. Jpn. **74** 1702 (2005).
[2] N. Oba, H. Kageyama, T. Kitano, J. Yasuda, Y. Baba, M. Nishi, K. Hirota, Y. Narumi, M. Hagiwara, K. Kindo, T. Saito, Y. Ajiro, and K. Yoshimura, J. Phys. Soc. Jpn. **75** 11360 (2006).
[3] Y. Tsujimoto, Y. Baba, N. Oba, H. Kageyama, T. Fukui, Y. Narumi, K. Kindo, T. Saito, M. Takano, Y. Ajiro, and K. Yoshimura, J. Phys. Soc. Jpn. in press.

Authors
H. Kageyama[a], Y. Tsujimoto[a], Y. Ajiro[a], K. Yoshimura[a], T. Fukui, Y. Narumi, and K. Kindo
[a]Graduate School of Science, Kyoto University

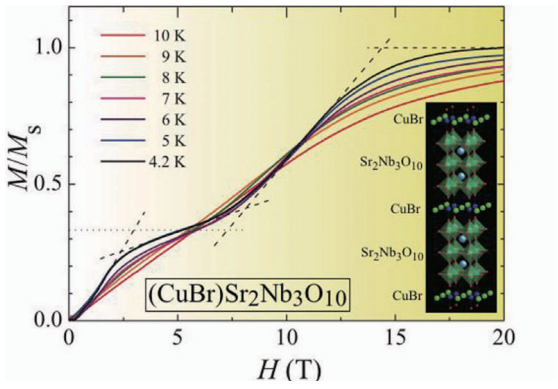

Fig. 1. Magnetization curves of single-crystal $(CuBr)Sr_2Nb_3O_{10}$. The inset shows the crystal structure $(CuBr)Sr_2Nb_3O_{10}$, in which the magnetic $(CuBr)^+$ layers constructing *S* = 1/2 square lattice are separated by the nonmagnetic $[Sr_2Nb_3O_{10}]^-$ perovskite slabs.

International Conferences and Workshops

10th ISSP International Symposium on Nanoscience at Surfaces

October 9-13, 2006
F. Komori

Research activities in nanoscience at surfaces have been significantly growing and taking advantages of accumulated knowledge of surface science. Previously, chemists in this field studied it as the useful ground of material formation, and physicists mainly progressed on the basis of the solid-state electron theory. Now the boundary between them should be broken down, and this interdisciplinary field is developing beyond the frame of each other's such as in the basic science of molecular conduction and atom/molecule manipulation. At the symposium, these were indeed two of the main topics.

This symposium was the tenth in a series of international symposia organized by ISSP every two or three years, and was co-organized as the University of Tokyo International Symposium 2006. A total of 242 scientific delegates from 14 different countries attended the symposium, and 210 papers were presented (19 invited and 21 oral contributions, and 170 posters). The symposium provided researchers in this field the opportunity to discuss properties of nanostructures on surfaces and their fabrication processes. Various advanced approaches were introduced for quantitative observations and elucidating the origins of newly discovered phenomena. The proceedings of the symposium is published as a special issue of Surface Science journal from Elsevier.

The tenth ISSP International Symposium (ISSP-10) on Nanoscience at Surfaces
9 - 13 October, 2006 Kashiwa, Chiba, Japan

ISSP International Workshop and Symposium "Computational Approaches to Quantum Critical Phenomena (CQCP)"

July 17 - August 11, 2006

N. Kawashima, T. Kato, Y. Tomita, S. Todo, and K. Harada

This is the first event of what the theoretical division at ISSP intends to be a series of small international meetings on condensed matter physics. While the main sponsor is ISSP, the symposium is also supported by I2CAM, an international organization that ISSP joined in 2005. The main objectives of the event were to survey the recent developments in computational physics and its applications to strongly correlated quantum systems, and to initiate discussions and new collaborations in these fields. In particular, we focused on the quantum critical phenomena, which have become tractable by various powerful numerical techniques developed in the last decade. The last three days (August 9-11) were dedicated to the symposium whereas the rest is for the workshop. Most of the participants stayed at campus during the workshop/symposium and intensive communications were developed among the participants. We invited 8 speakers from abroad and another 8 from Japan. During the workshop we had one or two lectures everyday. Typically there were 30 audiences present at the lectures. During the symposium, we had about 80 participants. The emphasis of the workshop was on the recent progress in algorithms, techniques and methods of computational condensed-matter physics. We also asked every invited speaker to make their lectures pedagogical so that graduate students can get sufficient information to start developing basic skills in this field. Topics covered include world-line quantum Monte Carlo, quantum Monte Carlo with dimer basis, density matrix renormalization group, exact diagonalization, dynamical mean-field theory, and new negative-sign free Monte Carlo method based on Gaussian basis. On the other hand, the symposium focused on new physics obtained from recent numerical calculations. We had 36 oral presentations and 19 poster presentations including not only computational works but also experimental and theoretical works. To name some of the most notable discussions, we had several impressive talks on (1) deconfinement critical phenomena, (2) supersolid, (3) ordering with magnetic quadrupoles or higher multipoles, and (4) field-induced magnetization and dimension reduction.

Taiwan-Japan Workshop on Neutron Scattering of Biomaterials and Soft-Matters for Nanotechnology and Biotechnology

December 7-9, 2006

M. Shibayama

The first Taiwan-Japan Workshop on Neutron Scattering was held in Tokai during the period of Dec. 7-9, 2006. In Taiwan, synchrotron X-rays are available for scattering studies. Besides X-rays, neutrons are very essential and irreplaceable probes for structural investigation of biomaterials and soft-matters. Japan is the most advanced country in neutron scattering in Asia and is now developing the next generation spallation neutron source, J-PARC, and neutron scattering instruments. In order to encourage future developments of neutron scattering facilities/researches in Taiwan, it was desired to develop more close research collaboration in applying the neutron scattering to these research fields. The objective of the meeting was to share the successful experience in applying the neutron scattering in Japan to study these interdisciplinary fields with Taiwan scientists for future neutron scattering researches of both countries. The research topics included nanomaterials, biomaterials (membrane, protein, peptides), and macromolecules (polymers). 44 Japanese and 12 Taiwanese scientists attended the meeting, and 24 oral and 14 poster presentations were given, covering interface, biology, polymer, soft-matter, hard-matter, and instrumentation. The meeting was quite successful and made an agreement to have the second meeting in Taiwan in 2007. This meeting was sponsored by Interchange Association, Japan, and Thaipei Economic & Cultural Representative Office in Japan.

ISSP Workshops

Electronic Properties of Nano-structured Organic Materials

April 24-26, 2006

K. Awaga, M. Yamashita, T. Matsumoto, H. Nishikawa, and H. Tajima

Electrical properties of organic materials have been studied extensively, and the research on organic semiconductors, metals and superconductors has been well developed, based on the detailed understanding on the correlation between the crystal/molecular structures and the bulk electrical properties. In recent years, organic semiconductors are attracting new attention as a component of organic electronic devices. This new research trend stimulates interdisciplinary studies of solid-state physics and chemistry, surface science, applied physics, etc., and is located on a crossing point between fundamental studies and applications. The present meeting consisted of invited and contributed talks and posters. We discussed various topics, such as organic thin films and their device applications, various electrical properties of nano-materials and biological materials.

New Progress of Studies on Phonons Responsible for Novel Properties

June 5-7, 2006

K. Iwasa, K. Hirota, O. Yamamuro, and I. Tsukushi

Studies of structural dynamics have recently been extended to biological systems, unconventional superconductors, disordered materials, as well as dielectric systems. These are strongly supported by rapid progress of experimental techniques investigating the atomic motions; inelastic x-ray scattering, terahertz time-domain spectroscopy, light scattering, nuclear resonance, neutron scattering, and so on. The various scientific topics, techniques and theoretical arguments to reveal the dynamical properties of material were gathered in this workshop that was held at the ISSP Kashiwa campus on June 5 - 7. The participants from the aforementioned different research fields exchanged information on the current research topics and discussed the future direction of phonon studies. We hope that this workshop will trigger interdiscipline of phonon science.

Water, Ice and Hydrogen: Earth and Space Sciences Meet Physics

October 24-25, 2006

H. Kagi, O. Yamamuro, T. Yagi, K. Aoki, E. Ohtani, T. Irifune, and K. Kakurai

The workshop attracted approximately 65 people to the ISSP Tokai campus on the basis of high-pressure science, earth and space science, solid state physics to discuss the properties of hydrogen-bearing materials at extreme conditions. It is worthwhile to note that many of participants are postdocs, graduate students and undergraduates. This implies that our science will further continue to expand in near future. It is obvious to use neutron as a probe to study hydrogen in materials. We learned that many efforts have to be made to develop new science in this field. Most of the participants also joined laboratory tours to J-PARC and JRR-3.

Fig. 1. Discussion at the workshop

Fig. 2. Laboratory tour at J-PARC

Unifying Concepts of Glass Transition —Interconnections of Theories and Assessment by Experiments—

November 20-22, 2006

T. Odagaki, M. Kataoka, T. Kanaya, H. Kawamura, M. Sasai, S. Shin, T. Suzuki, H. Takayama, K. Fukao, S. Fujikawa, J. Matsui, and O. Yamamuro

Glass transition is one of the most important unsolved problems of condensed matter physics. Since mid 1980's, understanding of glass transitions has progressed significantly due to advancement in experimental techniques and invention of the mode coupling theory (MCT), and now the research of glass transitions seems to have entered into a new stage. In fact, many international conferences and/or workshops have organized since 2000; to list a few, for example, International Discussion Meeting on Relaxations in Complex Systems (IDMRCS) in 2001 (Crete) and in 2005 (Lille), Workshop on Non Equilibrium Phenomena in Super-cooled Fluids, Glasses and Amorphous Materials (WNEP) in 2002 and 2006 (Pisa) and Unifying Concepts in Glass Physics (UCGP) in 2002 (Rome) and in 2004 (Bangalore). In these meetings, more and more emphasis has been put on the landscape picture than on the MCT.

In these moves in the world community, we have organized ISSP workshop in 2002 "New developments in glass physics" and in 2004 "Condensed matter in extremely non-equilibrium condition and energy landscape" in the Institute of Solid State Physics, The University of Tokyo, inviting active researchers in Japan.

In order to share new developments and advancements in the world in the community, we organized ISSP workshop "Unifying Concepts of Glass Transition". The scope of the workshop reads as:

> The main aim of this workshop is to give an opportunity for the participants to share new developments both in theory and experiment, by analyzing the current status of the research of glass transition in the world. We will make clear interrelations among theories such as the energy landscape and the MCT, and assess the plausibility of experimental tests of the theories. This will clarify what should be solved in theory and in experiment on the basis of the current understandings, which can be shared by all participants.

In the workshop, we had 158 participants from all over Japan (52 on 20th, 67 on 21st and 39 on 22nd), and 31 oral presentations and 13 poster presentations. From these beautiful presentations, we have learned that both theory and experiment on glass transitions have been progressing strongly. We also had very active discussions during the sessions and at the coffee breaks, and the workshop was successfully concluded with many outcomes formulating new themes and experiments.

Physics on Quantum Spin Systems

November 27-29, 2006

T. Sakai, H. Takayama, M. Takigawa, M. Oshikawa, H. Tanaka, and H. Kageyama

This workshop was held to search some new research fields on the quantum spin systems, and to activate comunication among different generations. It consisted of about 30 invited, 20 contirbuted oral presentations and 40 poster presentations. We focused on several hot topics; the nano magnets, chiral magnets, frustrated systems, spin liquids, Bose-Einstein condensation of magnons and Haldane systems etc. The discussions by young people after each talk were encouraged very much. As a result, more than 100 people participated the workshop every day and we had a lot ot fruitful discussions. We hope some young participants will hold a next interesting workshop in the near future.

For Establishment of a New Research Regime of the Condensed Matter Physics in Japan

December 7-8, 2006

M. Sato, Y. Kuramoto, Y. Murakami, Y. Suzumura, J. Akimitsu, Z. Hiroi, and H. Takayama

The proposal of the workshop was made by the chairman of the an unofficial research group of solid state physics in Japan to discuss various subjects brought about by rapid changes of research conditions or environments of universities and other research institutes after the introduction of the agency system to the universities and institutes. The introduction of a new system to the Science Council of Japan also seemed to give much influence on the research conditions. Many researchers actively working in the condensed matter physics participated in the workshop and constructive discussion was made on the subjects describe below.

(1) Roles and future planning of cooperative research institutes in Japan,
(2) Toward proper financial support for various researches in the condensed matter physics,
(3) Functions of the new Science Council of Japan and requests of the research group to the Council,
(4) To make the Japan Physical Society Meeting more effective,
(5) To raise the prestige of J. Physical Society of Japan,
(6) To support small-scale research groups, facing to difficulties induced by the new system,
and
(7) problems of the present post-doctoral system.

Supercomputer Utilization in the Computational Condensed Matter Science — Present and Future

December 11-13, 2006
O. Sugino, H. Takayama, K. Tsunetsugu, N. Kawashima, and S. Tsuneyuki

The users of the ISSP supercomputers and computational condensed matter scientists attended this meeting to present recent research activity and discuss future prospect. Since the last meeting of four years ago, the computer power has increased by more than a factor of ten and the computational approach has changed qualitatively. In a number of presentations, one could see new trend and progress in the research. There were sixty attendants and thirty two oral presentations. The meeting consisted only of oral presentations, without poster presentations and the party.

At the second day of the meeting, we held a special session regarding the future peta flops machine, which will be manufactured and served in five years from now. There we invited not only theoreticians but also experiments; we also invited an engineer who is engaged in manufacturing the peta flops machine. After the presentations and the discussions, the attendants have learned problems concerning the coming peta flops decade. The machine will necessarily be massively parallel machine that has narrow channels between CPUs, meaning that the computer code needs to adapt to the computational environment. The conversion of the code is very demanding and requires us to develop system to grow up more experts. Even after the efforts, there will remain problems on the condensed matter science that are not adapted to this computational environment.

At the end of the meeting there was request by an attendant that this kind of meeting should be regularly held.

Advances in Semiconductor Spintronics

December 14-15, 2006
S. Katsumoto and M. Tanaka

This ISSP workshop was held for exchange of most recent information on the research of spin-related physics and applications in semiconductor devices. The workshop was also announced to the community as "11th conference on Physics and Applications of Spin-related Phenomena in Semiconductors" (PASPS11).

In the workshop, "spin" can be either electron spin or nuclear spin. Actually the topics covers a wide range, *e.g.*, spintronics devices, material designs, spin-related theories, synthesis and characterizations of ferromagnetic semiconductors, nuclear-spin dependent transport, quantum manipulation of spins, and so on.

Three invited talks, one special report for making of "roadmap" in semiconductor devices, 26 oral talks and 32 posters were presented. Each session bore lively and sometimes heated discussion.

In the field of material science, several new ways to synthesize magnetic semiconductors with high transition temperatures were reported. The most impressive was the increase in the number of presentation on the nuclear spins. It is now clear that the transport in quantum Hall regime is strongly affected by nuclear spins under certain conditions. Thus electrical detection and manipulation of nuclear spins are prosperous now.

The next PASPS will be held in Osaka in 2007.

Electronic Properties of Pyrochlore Oxides

February 23, 2007
H Harima, M. Takigawa, and Z. Hiroi

This workshop was organized for understanding interesting electronic properties of pyrochlore oxides recently studied extensively. It attracted about 50 people including 11 guests from the outside of ISSP. Presentations on the superconductivity, Fermi surface and rattling of the beta-pyrochlore osmates were given in the first half of the workshop, and in the second half, various topics on the electronic properties and metal-insulator transitions of the alpha-pyrochlore oxides were discussed. Extensive discussions had been carried out through the workshop. It gave a wonderful opportunity to deepen and expand our knowledge on the pyrochlore oxides.